**An-Najah National University**

**Faculty of Graduate Studies**

# MODELING RUNOFF OF WADI AL ZEIMAR CATCHMENT CONSIDERING CLIMATE CHANGE

**By**

**Shahd Abdulhakim Yousef Bishawi**

**Supervisor:**

**Dr. Mohammad N. Al Masri**

**This Thesis is Submitted in Partial Fulfillment of the Requirements for the Degree of Master of Water and Environmental Engineering, Faculty of Graduate Studies, An-Najah National University, Nablus - Palestine.**

**2024**

# MODELING RUNOFF OF WADI AL ZEIMAR CATCHMENT CONSIDERING CLIMATE CHANGE

By

Shahd Abdulhakim Yousef Bishawi

This Thesis was Defended Successfully on 07/04/2024 and approved by

| | |
|---|---|
| Dr. Mohammad N. Almasri | |
| Supervisor | Signature |
| Dr. Fathi Anayah | |
| External Examiner | Signature |
| Dr. Anan Jayuosi | |
| Internal Examiner | Signature |

# Dedication

To my parents, I would want to dedicate this thesis. Many thanks for everything! I really don't know how to express how much I appreciate and thank you. You have served as my inspiration, pillar of support, and mentor. I've learned from you to be bold, tenacious, and self-assured. Having you as my parents makes me incredibly grateful and humbled. Thank you for everything. To take a quote from Albert Schweitzer, “At times our own light goes out and is rekindled by a spark from another person. Each of us has cause to think with deep gratitude of those who have lighted the flame within us.”

# Acknowledgements

"My Lord, increase me in knowledge." Quran-Verse (20:114)

I am grateful, to Allah, for His blessings that have helped me complete my thesis. I also acknowledge the guidance of our Prophet Muhammad SAW, who has contributed to the betterment of our lives today.

As I complete my thesis, I intend to send out my sincere thanks for all of the kind advice and help that many individuals have offered me.

I express my gratitude to my supervisor Dr. Mohammad N. Almasri, for his aid and support. In addition, I would like to express my deepest gratitude to the members of my defense committee for their invaluable guidance, support, and encouragement throughout this thesis.

I also thank my parents and brothers, for all the support and encouragement they have given me throughout my master's enrollment.

Special thanks and gratitude to my husband and son, who have been very helpful and understanding in my journey.

I would also like to express our gratitude to the Middle East Desalination Research Center (MEDRC), represented by Dr. Subhi Samhan, for their financial assistance through the Palestinian Water Authority (PWA) scholarship program.

# Declaration

I, the undersigned, declare that I submitted the thesis entitled:

**MODELING RUNOFF OF WADI AL ZEIMAR CATCHMENT CONSIDERING CLIMATE CHANGE**

I declare that the work provided in this thesis, unless otherwise referenced, is the researcher's own work, and has not been submitted elsewhere for any other degree or qualification.

**Student's Name:** **Shahd Abdulhakim Yousef Bishawi**

**Signature:** _____

**Date:** **07/ 04/2024**

# Table of Contents

# List of Tables

# List of Figures

# List of Appendices

# MODELING RUNOFF OF WADI AL ZEIMAR CATCHMENT CONSIDERING CLIMATE CHANGE

**By**
**Shahd Abdulhakim Yousef Bishawi**
**Supervisor**
**Dr. Mohammed N. Almasri**

## Abstract

Water covers a big portion of Earth's surface, but the availability of freshwater suitable for human use is limited. Scientists are focusing on hydrology and water resources management, with hydrological modeling gaining popularity for predicting water resource changes. Modeling helps understand processes like rainfall, evapotranspiration, infiltration, runoff, and underground water movement in the hydrological cycle. In regions like Palestine, intense storms can lead to flash floods due to primary precipitation processes. Climate change poses a significant challenge, as rising global temperatures are expected to alter hydrological processes, increasing the frequency of droughts and floods. To address flood risks and adapt to these changes, understanding the hydrological response to future climate change is crucial. This study integrated a hydrological model of the Al Zeimar catchment in Palestine with climate projections to assess the impact of future climate trends on watershed hydrology. The study used HEC-HMS 4.10 to model the rainfall-runoff relationship of the catchment, achieving reliable results with a Nash-Sutcliffe efficiency coefficient of 0.863. Climate change projections indicated rising temperatures, decreased precipitation, and increased maximum daily rainfall, heightening the risk of flash floods. Frequency analysis on maximum daily precipitation at the Nablus rainfall station from 1997-2022 forecasted a peak runoff of 92 $m^3$/second for a 25-year return period event, necessitating the redesign of a culvert at the entrance of Anabta Town. The culvert, initially sized at 10 $m^2$, was enlarged to 30 $m^2$ to withstand the expected storm intensity. However, this solution is not feasible nor applicable. Recommendations included further assessment of other culverts in the town, and searching for solutions other than enlarging culverts.

Keywords: Hydrologic Modeling; Run-Off; Wadi Al Zeimar; Climate Change;

# Chapter One

# Introduction and Theoretical Background

## 1.1 General Background

During a rainstorm, the question “What happens to the rain?” might come to mind. In 1961 Penman listed Hydrology as the branch of science that seeks to answer this question (Singh & Woolhiser, 2002). Rainfall is part of the hydrologic cycle. The term cycle suggests that water is generated from one source and ultimately finds its way back there. Oceans are the source and last destination of water. Ocean water evaporates and turns into atmospheric water vapor. A portion of the moisture present in the atmosphere is released as precipitation, which occasionally evaporates before it reaches the ground's surface. Some of the water brought to the Earth’s surface by precipitation may evaporate on site while some might seep into the ground and some could flow across the land to form streams. Once water has seeped into the earth, it can evaporate, seep below to groundwater reservoirs, or be absorbed by plant roots and then transpired by the plants. When water enters groundwater reservoirs, it can either flow straight into streams or the ocean, or it can migrate laterally until it gets near enough to the surface to be exposed to transpiration or evaporation. It can also reach the land surface and produce lakes, seeps, or springs. Flowing stream water can condense in lakes and surface reservoirs, seep into groundwater reservoirs, evaporate or be transpired by riparian plants, or return to the ocean, where the cycle starts all over again (ASCE, 2013). In this study, rainfall is the most significant process. The main element influencing the hydrology of wadi systems in this study is rainfall. In arid and semi-arid locations, wadi systems are frequently affected by irregular storms which fluctuate significantly in terms of both time and location. The part of rainfall that enters wadi channel systems after infiltration, detention storage, and other abstractions are met is known as direct runoff, or storm flow. Surface runoff, which begins as a thin layer of sheet flow known as overland flow, is frequently the predominant runoff pathway because of high rainfall intensities and sparse vegetation. This overland flow becomes concentrated and changes into channel flow when it approaches a wadi or canal. Flood flows typically lose water by infiltration into the channel bed in dry and semi-arid regions. These losses are referred to as transmission losses. These losses may decrease channel flow while approaching downstream

(Weshah, 2010). Understanding all the above is essential and can be achieved through modelling.

Simplified representations of real hydrologic systems, known as hydrologic models, help better understand hydrologic processes through studying the functioning of watersheds and their response to different inputs (Verma, Jha, & Mahana, 2009) . Watershed hydrological models are designed to answer Penman's question at a specific level of detail depending on the problem at hand (Singh, Computer Models of Watershed Hydrology, 1995). The availability of adequate data to accurately represent each of the modeled processes is a fundamental need for any physically based model. Geospatial technologies, including geographic information systems (GIS), global positioning systems (GPS), and remote sensing, are enabling significant advancements in data collection, preparation, and administration (Daniel, et al., 2011). (Beckers, Smerdon, & Wilson, 2009) suggest that a crucial element to enhance the performance of hydrologic models is to properly quantify climate change, which includes potential future changes in temperature and precipitation, the occurrence of severe events, and changes in glacier mass balances. Climate change is widely acknowledged as the biggest environmental issues the world is now facing (Parry, Canziani, Palutikof, Linden, & Hanson, 2007). According to Eltahir and Pal (2022), future temperatures in the Middle East are predicted to rise, leading to increased evapotranspiration and potential changes in climatic patterns resulting in reduced overall rainfall in the region. On the other hand, recent studies indicate that the Eastern Mediterranean area is projected to experience an increase in extremely heavy daily rainfall and a decrease in annual precipitation as a result of global warming (Almazroui, Islam, & Jones, 2023). The Mediterranean climate is often characterized by its irregular rainfall patterns, which may aggravate water stress during specific times and lead to a period of water scarcity (Ceballos, Fernandez, & Ugidos, 2003). A climate change study in Israel (Historic Palestine) concluded that by 2050, mean temperature will escalate by 0.7º-0.8ºC and there will be a drop in precipitation by 4 % to 2% (Pe'er & Safriel, 2000).

Palestine is made up from 33 watersheds where one of them is the well-known Al-Zeimar watershed. Al Zeimar stream runs from the hills of Nablus in the West Bank to the coastal region of Tulkarm and discharges into the Mediterranean Sea. The watershed is made up of a variety of land use and land cover types including built-up areas (for instance the

western part of Nablus City). The built-up areas are responsible by large in the generation of the surface runoff at high rates. Due to that, and in addition to climate changes, the watershed encountered in the past many incidents of flooding that did lead to catastrophic consequences of infrastructure damage and death causalities. In January of 2013, two young girls lost their lives due to the flooding of Al Zeimar in Anabta area in Tulkarm. This fatal event was a shock to the community, because nothing similar occurred in decades before. The culverts in the area are usually partially blocked because residents dump everything there. This, in addition to the powerful storm, knocked down trees into the path of the culvert, which lead to backflow and flooding of the area. This thesis aims at assessing the impact of climate change on flood hazard in Al Zeimar. To achieve this purpose, the hydrological model of the catchment was developed using HEC-HMS (Hydrologic Engineering Center-Hydrologic Modeling System). After the model was calibrated and validated, it was used to project the climate change shifts in the study area. Moreover, a culvert at the entrance of Anabta Town was tested for peak flow and re-designed to handle a 25-year return period storm.

## 1.2 Objectives

The following are the objectives of the research:

- To model the rainfall-runoff generation of Wadi Al Zeimar using HEC-HMS
- To simulate the effect of future climate changes on the runoff generation in the study area
- To redesign the culvert at the entrance of Anabta using HY-8 based on the runoff value from HEC-HMS under future climate changes

## 1.3 Research Questions

In light of the identified objectives, this research aimed to answer the following questions:

- What are the key factors and methodologies necessary to develop a reliable and representative hydrologic model for Al Zeimar catchment?

- How do climate fluctuations contribute to the occurrence of extreme flood events in Al Zeimar catchment?

- What are the operational capabilities of the culvert at the entrance of Anabta in Al Zeimar during extreme flood events?

### 1.4 Research Motivations

Several factors contributed to giving this research a great importance, listed from them are the following:

- This study is the first to model the runoff of Al Zeimar catchment considering climate change
- The HEC-HMS model of Al Zeimar catchment, is the only calibrated and validated model of the catchment based on real run-off data.
- The study area has many features that led to choosing it, as in the following:
  a. The wadi runs by a good number of human communities.
  b. The wadi passes by several water sources, such as the Anabta Well.
  c. A flash flood occurred in this catchment in 2013 and caused a lot of damage and loss of life.
  d. The wadi of the catchment is transboundary. It starts from the hills of Nablus, passing by Tulkarm then the green line, and pour into the Mediterranean.

### 1.5 Literature Review

Al Zeimar catchment has always been a study area of interest for researchers. Previous studies, such as the study conducted by Ahmad (2014) , mainly focused on the quality of the discharge in Al Zeimar wadis because they suffered from several sources of pollution; effluents that enter the stream through the wadi beginning with deposition of raw sewage from the western side of Nablus wastewater addition to agricultural and industrial pollution (Darawosheh, 2014). In 2013, Nablus Waste Water Treatment Plant was launched to treat wastewater from the upstream wadis to protect surface and ground water sources from pollution, and to eliminate the diseases and odors due to the flowing wastewater in Al Zeimar wadi (Palestinian Water Authority (PWA), 2024). Few research outlined the hydrological assessment of the catchment's wadi and the development of the rainfall-runoff relationship that is fundamental for catchment management and an essential tool in future flood prediction.

Zayed, Qutob, and Almasri (2011) conducted a study in the West Bank focusing on Wadi Al Zeimar in Anabta Their objective was to address the challenges within the Wadi,

engage stakeholders, and forecast potential flood-related issues. They measured the wastewater generated from western Nablus and nearby villages during summer using water level monitoring devices at wadi culverts. For the winter season when stormwater mixes with wastewater, they estimated the flow synthetically employing the SCS (Soil Conservation Service) Unit Hydrograph method. By developing a flow hydrograph of Al Zeimar, they constructed a flood map to pinpoint critical sections. Their recommendations included advocating for further research to expand the study area and implementing regulations to curb garbage dumping in the wadi.

Hammad et al (2011) derived a synthetic unit hydrograph for Al Zeimar using the SCS Synthetic Unit Hydrograph method, chosen for its reliance on the physical characteristics of the watershed. Notably, at the time of the study, the catchment remained ungauged. Meteorological data were sourced from Nablus and Tulkarm metrological stations as well as municipalities. The synthetic unit hydrograph generated for a 1-cm rainfall event resulted in a flow peak of 21.65 $m^3/s$, a substantial figure given the magnitude of rainfall. An alternative approach, Snyders Method, necessitating similar data as SCS, yielded a significantly higher flow peak of 184.15 $m^3/s$. It was recommended that flow measurement instruments be installed in catchment wadis to acquire authentic runoff data, facilitating the development of a rainfall-runoff model for the catchment

In 2013, a catastrophic event that changed the focus of the direction of research in the catchment occurred. It all started when the region woke up to a rainy day on the $6^{th}$ of January, nobody suspected anything. The water level raised as usual in Al Zeimar catchment. Suspicions started rising when the intensity of the rainstorm increased, and was continuous. On the $7^{th}$, the rain water started seeping into the houses around the wadis. The fatal event occurred on the $8^{th}$ of January, the culverts in the Anabta section of the catchment were completely clogged and the area flash flooded. The flood destroyed everything on its way, from cars, trees, and infrastructure, but the biggest loss was the lives of two young ladies who were trapped in a taxi, and got swept by the flood (AQUA Consulting Center, 2013). The storm was called Alexa with substantial precipitation in the form of both rain and snow, it was the worst storm to hit the area in 60 years (ICRC, 2021). In the summer of the same year, AQUA Consulting Group studied the rehabilitation of Al Zeimar' culverts. This project came as a direct response to the flood and its disastrous consequences. The implementation of studies related to

the project were proceeded in several steps: the first was an attempt to understand what happened in a scientific manner based on accurate data and special mathematical models, the second was to evaluate the status of the wadi and the existing culverts in terms of their ability to drain surface runoff from different rain storms, and the third was to develop proposals and solutions consistent with the reality of the valley, its characteristics, ownership boundaries, and the nature of the surrounding buildings, and fourthly, the structural design of culverts and any other facilities that could be affected by the new situation, such as: streets. After data collection and analysis, they developed a HEC-HMS model to study the rainfall-runoff relationship in the catchment. It is important to note that there was no real runoff data at that time, so the model was neither calibrated nor validated. The model simulated the storm that occurred between the 6$^{th}$ and the 8$^{th}$ of January 2013, and resulted in a simulated peak flow of 75 $m^3/s$ at the wadis outlet. Peak flows on Anabtas' culverts were used in HY-8 (Culvert Hydraulic Analysis Program), to redesign the culverts, for the fatal storm, and storms with return periods of 10 years. They recommended that the wadis culverts be continuously cleaned, because trash partially clogged them and decreased their drainage capacity. Furthermore, they recommended that all the culverts should be enlarged (AQUA Consulting Center, 2013).

According to the United Nations Development Program (2020), the Climate Change Profile for Palestinian Territories highlighted forecasts of climate change that showed a significant rise in temperature and a drop in the amount of precipitation that falls on a yearly basis. In addition, they predicted that by the end of this century, an increase in temperature ranging from 1.8° to 5.1° is probably to take place. Yearly rainfall rates are likely to drop by 10% in 2020, by 20% by 2050, and may reach a drop of 35% by 2100 with a high risk of summer droughts. Additionally, a significant decrease in the length of cold spells and a significant rise in the duration of heat waves are predicted. Regarding flooding, flash floods are more likely to be caused by High Precipitation Events (HPEs) and rainfall variability.

Shadeed performed a trend analysis of temperature and precipitation data for the Nablus Metrological Station (NMS) in the West Bank, Palestine, in 2013. It was determined through rainfall studies that the NMS has highly variable rainfall, with an average annual rainfall of 654 mm and annual variations of from 335 to 1,400 mm. Rainfall is generally trending toward a wetter environment, with an estimated 48 mm rise over the course of

the study period. With an average temperature of 18.4°C and a standard deviation of 0.8°C, the temperature variability between years (1975-2011) was demonstrated through the analysis of temperature. It was concluded that the changes in climate of NMS are considerable and largely affect the sustainable yield of the water resources in the West Bank (Shadeed, 2013).

Assaf et al. (2018) obtained high-resolution climate projections over Israel with the regional model COSMO-CLM. For the years 2041–2070, the simulation offers high-resolution spatial variability of total precipitation and intensity. The forecasts indicated that seasonal mean temperatures will generally rise over the domain, peaking at 2.5°C, particularly in the winter and fall. The extreme temperature index indicates a rise, with a higher lowest temperature than a higher maximum temperature. There were drops of up to 40% in the overall amount of seasonal precipitation in Israel's central Mediterranean climate.

# Chapter Two

# Materials and Methods

## 2.1 Study Area

### 2.1.1 Location

Al Zeimar catchment lies in the West Bank, Palestine. It is located in the North-West, and in one of the 33 catchments of the West Bank. The catchments' streams are transboundary streams, where they originate in Nablus, and flow towards Tulkarm. The streams cross the 1949 Armistice Agreement Line flowing through historic Palestine, then drain into the Mediterranean Sea. The total watershed area is 600 $km^2$ where 172 $km^2$ are on the Palestinian land. The total length of Al Zeimar stream is 50 km where 27 km flow in the Palestinian area. The average inclination is about 1.2% in the first 10 km and 0.9% in the remaining length (Dotan, et al., 2017) , (Becker, Friedler, & Haddad, 2007) . The altitude of the catchment varies from 75 m amsl (above measured sea level) in the plain of Tulkarm to 925 m amsl in the mountains of Nablus. Figure A.1 in Appendix A shows the map of the location of Al Zeimar catchment within the West Bank, and shows the digital elevation model of the catchment.

### 2.1.2 Population

The Zeimar catchment lies within two main cities, Nablus and Tulkarem. Nablus has a population of 174387, and Tulkarm has a population of 71161 people according to population statistics by (Palestinian Central Bereau of Statistics PCBS, 2023). PCBS??? Other medium sized towns also contribute to the flow of the river. Figure A.2 shows the communities within the catchment. Table B.1 shows the communities within the catchment.

### 2.1.3 Geology

The Wadi Al Zeimar research region contains geological strata that span the Senonian to Quaternary ages. The catchment region is mostly covered by sedimentary carbonate rocks like chalk, dolomite, limestone, and marl (ARIJ A. , 1996).

### 2.1.4 Soil Cover

The majority of land is covered by loose surface material called soil. Soil is made up of both organic and inorganic materials. In addition to being a source of water and nutrients, soil gives agricultural plants the structural support they need (Leeper & Uren, 1993). Table B.2 summarizes the soil cover of the catchment(Rofe and Raffety Consulting Engineers, 1965) (ARIJ A. , 1996). Figure A.3 in Appendix A shows the spatial distribution of soil over the catchment.

### 2.1.5 Land Use

As for the land use within Al Zeimar catchment, Table B3 in Appendix B shows the different land use types and their areas within the catchment. Figure A.4 in Appendix A shows the distribution of the land use types over the catchment.

### 2.1.6 Wadis

Wadis are naturally occurring waterways that remain dry for the majority of the year. They temporarily transform into conveyors of runoff during wet seasons, primarily during and after a heavy rainfall. Surface runoff does not generate with every storm. Permanently flowing water often exists in the gravels below the surface of a large wadi subsurface terrain (Sen, 2008). Figure A.5 in Appendix A shows the wadis in Al Zeimar Catchment. Table B.4 in Appendix B shows the wadi corresponding to each ID.

In the dry season, the flow in the wadi is mainly treated wastewater. The Nablus WWTP shown in Figure A.5 is located near Beit Leid. The wastewater is collected from western Nablus and from five villages namely; Zawata, Beit Eba, Beit Wazan, Deir Sharaf and Qusin. One of its main purposes is to improve the environmental and health conditions in upper wadi Zeimar (ID 0 in Figure A.5). The treated wastewater discharge from the treatment plant varies from 10,000 $m^3$/day and 14,000 $m^3$/day (Abu Jafal, Hmeidan, Bitar, & Abu-Salameh, 2023). Wastewater from almost all communities in the wadi is conveyed in closed sewage systems, except for almost 100 residencies in Anabta that are not connected to the main sewage line, causing the treated wastewater to mix with untreated wastewater in the wadi. In addition, olive mill waste is dumped in the wadi especially in October and November. In the rainy season, the direct runoff in Al Zeimar wadi is approximately 23,800 $m^3$/day (ARIJ A. R., 2015).

### 2.1.7 Climate

There are 5 main climatic zones in the West Bank. Al Zeimar catchment is located in the Central highland's region which lies 400 to 1000 m amsl, and has an annual rainfall that varies between 300 mm in the south to 600 mm in the north (Climate Change Profile - Palestinian Territories, 2020). The weather conditions of the basin are typical East Mediterranean. The East Mediterranean climate conditions are branded by moderate air temperatures during the rainy winter season and dry and stable hot weather conditions during summer (Hochman, Mercogliano, Alpert, Saaroni, & Bucchignani, 2018). The spatial distribution of the climatic features is affected by topographical and coastal effects. Such effects are immediately noticeable in the mountainous areas (Hochman, et al., 2017) . There are two main weather stations in Al Zeimar, one in Nablus and the other one in Tulkarm. Each station measures the following parameters:

- Daily Rainfall
- Evaporation
- Relative Humidity
- Wind Speed
- Air Pressure

As for the station's locations, Nablus station is located at a longitude of 35°15' E and a latitude of 32°13' N, with an elevation of 570 meters above sea level. In contrast, Tulkarem station is situated at a longitude of 35°01' E and a latitude of 32°19' N, with a much lower elevation of 83 m amsl. (Palestinian Meteorological Department, 2024).

### 2.1.8 Temperature

- The coldest months of the year extend from October – April, and the hottest extend from May – September. Temperatures in winter range from 8 to 14 °C, while the summer temperatures range from 21 to 40 °C (Becker, Friedler, & Haddad, 2007). Figure A.6 in Appendix A shows graphs of the average annual temperatures for the coldest and hottest months of the years 2007 – 2018 for the Nablus station (Palestinian Meteorological Department, 2024) (The Nablus station was used because the Tulkarem station has data gaps. The following are the general comments about the hot months (2007-2018) :

- The average temperature during the hot months fluctuates between approximately 21.5 and 23.5°C.
- The lowest average temperature appears to be around 21.5°C, occurring early in the data range (likely in the late 2000s).
- There is a noticeable peak in the middle of the chart, with the temperature reaching approximately 23.5°C, indicating a significant increase compared to the initial years.
- Following the peak, there is a slight decline but temperatures remain higher than the initial years.
- Towards the end of the range, there is another rise, with temperatures reaching near the peak values.

As for the cold months (2007-2022), the following are the general comments:

- The average temperature during the cold months fluctuates between approximately 11.0°C and 16.5°C.
- The lowest average temperature is around 11.0°C, appearing early in the data range (likely in the late 2000s).
- There is a significant peak reaching around 16.5°C in the middle of the chart, showing a substantial increase compared to other years.
- Post the peak, temperatures drop again but not as low as the initial years.
- Towards the end of the range, temperatures rise again, indicating another significant increase.

### 2.1.9 Rainfall

The year in Palestine is classified into two seasons: the rainy season and the dry season. Rain casually begins early in November, and ends late April. The span flocculates greatly between years. There are plenty of sunny days during the rainy season as well. One or more days of rain are followed by a stretch of beautiful weather. Rainfall usually lasts for five days, although occasionally it might last for 10 or fifteen days (Rice, 1886). Precipitation in arid and semi-arid regions is generally identified by extremely high spatial and temporal variability (Whaeater & Al-Weshah, 2002). Figures A.7 and A.9 in Appendix A shows the graphs of the average annual rainfall in mm, and Figure A.8 shows the number of rainy days for the Nablus and Tulkarm stations from (2007 – 2018). The average annual rainfall in Nablus is 660 mm. From the chart of Figure A.7 in Appendix

A it can be seen that the average rainfall values are very flocculant, which is the general is a characteristic of semi-arid regions. After 2013, it is observed that the average annual rainfall decreased, while the number of rainy days increased, and this supports the predicted climate change scenarios for the study area. The graph in Figure A.9 in Appendix A shows average annual rainfall for Tulkarem station. The average annual rainfall in Tulkarm is 602 mm. It is notable that the amounts of rainfall in Nablus are generally higher than in Tulkarm. In addition, in 2013, there was an extreme rainfall event that led to fatal consequences, and this can be seen from the big rainfall values over the same average of rainfall days in 2013 for both Nablus and Tulkarem. The map labeled Figure A.10 Appendix A shows the map of the rainfall contours of the whole catchment, the rainfall contour shapefile was retrieved GEOMOLG spatial database (Government P. M., 2023).

### 2.1.10 Climate Change

Climate change may cause significant seasonal swings or changes in rainfall in some parts of the world. Thus, it is essential to do research into how various hydrologic components are affected by climate change (Abbas, Zhao, & Wang, 2022). This might lead to more frequent water shortages, flooding, and problems with food security. The hydrologic cycle is impacted by climate change in ways that affect soil moisture, evapotranspiration, and precipitation (Abbas, Zhao, & Wang, 2022). Understanding climate disorder commonly involves establishing a hydrological model set by taking into account various simulations through a series of global climate models (GCMs) (Christierson, Vidal, & Wade, 2012). To downscale climatic data from global scale to catchment scale, the chain “GCM–RCM (Regional Climate Models)–HM (Hydrologic Models)” is efficient for scenario-based data collected by downscaling (Fonseca & Santos, 2019). Despite the fact that climate change is not a pressing issue to the Palestinian, the climate risks are noteworthy due to the limited capacity to respond to the effects of climate change (Climate Change Profile - Palestinian Territories, 2020). Climate trends from recent and projected models reveal that temperatures in the area will increase, precipitation will decrease, and high precipitation events (HPE) will happen. Hochman et al. (2018) obtained high resolution climate projections over Israel for the period 2041-2070 with the regional model COSMO-CLM. The climate projections obtained from the previous study were used in this study to simulate the future climate

shifts using HEC-HMS. It is significant to remember that the use of global climate models to simulate the intricate climate regime of the Mediterranean region has drawn criticism (Lionello, Gacic, Planton, Trigo, & Ulbrich, 2014). To bridge the gap between GCMs and simulations of local climatic variables, the dynamic downscaling approach was used in the previous study. The temporal distribution of daily rainfall data is used to assess the environmental impacts of short-term phenomena climate change processes (Zhang, et al., 2011). The future projections of Hochman's' study assumed that greenhouse gases will increase and peak around 2040, and then will start to decline (Moss, et al., 2010). The extreme precipitation indices (EPI) (The unit is mm/day) are:

- SDII: Mean Precipitation on wet days (> 1 mm)
- Rx 1day: Maximum of daily precipitation
- 99p: $99^{th}$ percentile of daily precipitation
- 90p: $90^{th}$ percentile of daily precipitation

The projections for the EPI for the period of 2041-2070 were made for the whole country (Palestine), the following results show projections specifically over the study area of Al Zeimar catchment according to (Assaf, Paola, Pinhas, & Hadas, 2018) ???

- SDII is projected to decrease in Al Zeimar catchment by almost 1 mm/day.
- Rx 1 day is projected to increase by almost 12 mm/day.
- The 99 p is projected to increase by almost 14 mm/day.
- The 90 p is projected to decrease by almost 3 mm/day.

### 2.2 The Methodology

The methodology can be divided into five major tasks:

- Data collection and analysis
- HEC-HMS model development
- HEC-HMS model calibration and validation
- Projection of the EPI to simulate climate change
- Redesign of the culvert at the entrance of Anabta using HY-8

### 2.2.1 Data Collection and Analysis

In any system, the quality of the output is determined by the quality of input (Awati, 2015). Wherefore for the HEC-HMS model to be able to generate reliable results, the input data should be precise and representative. The following are the data required to create the inputs for the model:

#### 2.2.1.1 Ground Surface Contours

Contours are needed to develop the Digital Elevation Model (DEM) of the study area. DEM is the digital representation of the land surface elevation with respect to a reference datum (Balasubramanian, 2017). The 25 m contours of the study area were extracted from (Government P. M., 2023) a GIS shapefile, and then were processed in ArcMap 10.8 using the 3D Analyst.

#### 2.2.1.2 Lag Time

According to the Hydrologic Modeling System HEC-HMS: Technical Reference Manual (2022) , a unit hydrograph is a discharge hydrograph resulting from 1 unit of direct runoff distributed uniformly over the catchment that result from a rainfall of a specified time span. The unit hydrograph procedure assumes that discharge at any time is directly proportional to the volume of runoff and that time factors affecting hydrograph shape are constant. The SCS unit hydrograph method makes use of a dimensionless, curvilinear unit hydrograph to route excess precipitation to the watershed outlet. This dimensionless, curvilinear unit hydrograph expresses discharge, (q), as a ratio of the peak discharge ($q_p$) for any time (t), as a fraction of the time of rise, ($T_p$). The following summarizes the related equations:

- $T_p$ can be related to the duration of excess precipitation as :

$$T_p = \frac{t_r}{2} + t_p \qquad (1)$$

  - $t_r$: duration of excess precipitation (or computational time step)
  - $t_p$: the basin lag time which is defined as the time difference between the center of mass of excess precipitation and the peak of the unit hydrograph
- The unit peak discharge $Q_p$ for 1-cm of excess rainfall (Feldman & Hydrologic Engineering Center U.S, 2022):

$$Q_{p=}2.08\left(\frac{A}{T_p}\right) \quad (2)$$

where A is in ($km^2$,) $Q_p$ in ($m^3/s$), Tp in (hr)

- To utilize the SCS Unit Hydrograph method, the basin lag time is needed, it is estimated to be:

$$t_p = 0.6T_c \quad (3)$$

- $T_c$: Time of concentration, longest travel time that it takes surface runoff to reach the discharge point of a catchment

The Kirpich Formula was used to find the time of concentration:

$$T_c = 0.01947L^{0.77}S^{-0.385} \quad (4)$$

- Tc: time of concentration in (min.)
- L: Maximum length of travel water (m)

ΔH: Difference in elevation between the most remote point on the catchment and the outlet (National Engineering Handbook, 2021). HEC-HMS automatically calculates L, S, and ΔH after the watershed is delineated.

#### 2.2.1.3 Land Use / Land Cover (LULC) and Soil Maps

According to the National Engineering Handbook (2021), the terms "land cover" describes the surface cover of the earth, including bare soil, water, plant, and urban infrastructure. The term "land use" describes the use of the land, such as agriculture, wildlife habitat, or recreation. When coupled with the term "Land Use/Land Cover," (LULC) typically denotes the classification of both natural and human-made features on the terrain during a given period of time (SATPALDA, 2018). LULC maps are used with the soil map of the catchment, to identify the NRCS-CN (previously named SCS-CN) input parameters for the model. The NRCS-CN method, is a method used to estimate runoff volume resulting from a storm event. The NRCS runoff equation, according to the National Engineering Handbook (2021):

$$Q = \frac{(P-0.2S)^2}{(P+0.8S)} \quad \text{For } P > Ia \qquad (5)$$

$$Q = 0 \qquad \text{For } P \leq Ia \qquad (6)$$

- Q = Runoff (mm)
- P = Rainfall (mm)
- $I_a$ = Initial abstraction (mm)
- S = Potential maximum retention after runoff begins (mm)

Initial abstraction (Ia) includes all losses (water retained on the landscape) before runoff begins. It includes water retained in surface depressions, water intercepted by vegetation and other cover, and water lost to evaporation and infiltration. Ia is highly variable but is generally correlated with soil and cover parameters. Through studies of many small agricultural watersheds, researchers found Ia to be approximated by (United States Department of Agriculture, 2021):

$$I_a = 0.2S \qquad (7)$$

The potential maximum retention, S, can range from zero on a smooth, impervious surface to infinity in deep gravel

$$S\ (mm) = \frac{25400}{CN} - 254 \qquad (8)$$

Runoff curve numbers (CN) can be any value from zero to 100, but for practical applications it is within a limited range of about 40 to 98. Researchers developed the runoff curve numbers in Table B.5 in Appendix B by examining rainfall runoff data from small agricultural watersheds. These values were sourced from the USDA's National Engineering Handbook (2004) The runoff curve number for a given soil-cover type is not constant but varies from storm to storm, and even within the storm (United States Department of Agriculture, 2021). The NRCS-CN method assigns a representative runoff curve number for a given soil and cover type for design purposes. The NRCS defines four hydrologic soil groups that, along with land use, management practices, and hydrologic conditions, determine a soil's associated runoff curve number. The classification shown in Table B.6 in Appendix B. These values were also sourced from the USDA's National Engineering Handbook (2004). When the model is used for event-

based flood prediction, the AMC becomes a vital factor affecting runoff production (Bahremand & De Smedt, 2006). The AMC values in Table B.7 is determined according to the sum of all precipitation for the 5 days and the season (dormant or growing) (Mihalik, Levine, & Amatya, 2008).

The CN are for AMC II. The CN values for dry soil (AMC I) or saturated soil (AMC II) are calculated using the following formulas (Luijten, Jones, & Knapp, 2002) :

$$CN\text{I} = \frac{(-75 * CN\text{II})}{(-175 + CN\text{II})} \; For\ AMC\text{I ( Dry Soil)} \tag{9}$$

$$CN\text{III} = \frac{(175 * CN\text{II})}{(75 + CN\text{II})} \; , For\ AMC\ \text{III ( Saturated Soil)} \tag{10}$$

For the sub-catchments within the watershed that have different soil types and land covers, a composite $CN_c$ is determined by weighting the curve number values for the different sub-areas in proportion to the land area associated with each (Shadeed, Hydrologic Analysis, 2019) :

$$CNc = \frac{CN1A1 + CN2A2 + \cdots . + CNiAi .. + CNnAn}{\sum_{i=1}^{n} Ai} \tag{11}$$

After the land use and soil type shapefiles are obtained, they can be compiled in a GIS based database. For land use, the area of each subclass was calculated. For soil type, the Hydrologic Soil Group (HSG) was assigned for each soil type. It is important to note that the study area is made up of clay loam (C) and clay (D). Both shapefiles were intersected, and the attribute table of the resulting shapefile was exported to MS Excel (Easier to process the data because GIS requires Python). The CN for each sub-basin was assigned by the methodology shown in the flow chart in Figure A.11 in Appendix A.

#### 2.2.1.4 Channels' Average Cross Section and Properties

According to information on the HEC-HMS Tutorials and Guidelines website (U.S. Army Corps of Engineers, 2022) , the hydrologic network is made up of various elements, one of them is the reach. It simulates a part of a stream or river. Flood routing is a method to calculate flow depths, velocities, volumes, and discharges at a river section. When a flood wave enters a river upstream section, using flood routing one can detect

the movement of flood wave along a channel length and thereby can calculate flood hydrograph at any downstream section of the river. The conservation of mass is the main principle of the routing methods. They require important field data, such as cross-sectional surveying, roughness, flow depth and velocity measurements (Tayfur, 2023). The Muskingum flood routing method is one of the most common hydrological approaches. Using the mass-conservation equation this method defines the channel storage in each time interval as a function of the inflow entering the channel and the outflow exiting the channel (Niazkar & Zakwan, 2022). The equation of the total storage in the channel reach is :

$$S = KQ + Kx(I - Q) \quad (12)$$

- S: Storage ($m^3/s$)
- I: Inflow Discharge ($m^3/s$)
- Q: Outflow Discharge ($m^3/s$)
- K: Time of travel of the flood wave through the channel reach (sec)
- x: Value that depends on the shape of the wedge, in natural stream it varies from 0 and 0.3

To apply the Muskingum Routing method in the HEC-HMS model, k and x should be defined.

- K is the travel time through the reach. Its initial value is estimated by comparing flow length to a flood wave velocity (U.S. Army Corps of Engineers, 2022) *:*

$$T = \frac{L}{V_w} \quad (13)$$

- T: Travel time of a flood wave (sec)
- L: Length of the reach (m)
- $V_w$: Flood wave velocity (m/s)

The flood wave velocity is estimated using Mannings Equation. It is one of the most commonly used equations governing open channel flow. The Mannings equation is an empirical equation that applies to uniform flow in open channels and is a function of the

channel velocity, flow area and channel slope (Hydraulic Reference - Manning Equation, 2004) :

$$Q = VA = \left(\frac{1}{n}\right) AR^{2/3}\sqrt{S} \qquad (14)$$

- Q = Flow Rate ($m^3/s$)
- V = Velocity (m/s)
- A = Flow Area ($m^2$)
- n = Manning's Roughness Coefficient
- R = Hydraulic Radius (m)
- S = Channel Slope (m/m)

The Manning's n is a coefficient which represents the roughness or friction applied to the flow by the channel. Manning's n-values are selected from Table B.8 in appendix B.

The roughness coefficient values were retrieved from the Handbook of Hydrology (2019)

To find the initial value of K, the equation becomes

$$V = \left(\frac{1}{n}\right) R^{2/3}\sqrt{S} \qquad (15)$$

The initial estimation of the previous equations' parameters was done through field visits, and using aerial photographs of the study area. For x, great accuracy in determining it may not be necessary because the results of the method are relatively insensitive to the value of this parameter (Shadeed, Hydrologic Analysis, 2019).

### 2.2.2 Model Development

The hydrologic model of the watershed was simulated using HEC-HMS 4.10[1]. HEC-HMS (Hydrologic Engineering Center-Hydrologic Modeling System) was developed by the United States Army Corps of Engineering (USACE). The software is a generalized modeling system that can simulate a wide range of watershed types. It is a mathematically based (conceptual) deterministic semi-distributed event-

[1] https://www.hec.usace.army.mil/software/hec-hms/

based/continuous model. By breaking down the hydrologic cycle into smaller, more manageable components and drawing boundaries around the watershed of interest, a model of the watershed is created (Feldman & Hydrologic Engineering Center U.S, 2022). The components of a HEC-HMS model are:

- Terrain Data
- Basin Model
- Meteorological Model
- Time-Series Data
- Control Specifications

HEC-HMS was used for the hydrologic modeling of Al Zeimar for various reasons. First it allows for the simulation of precipitation-runoff processes, which can be crucial for understanding flood forecasting, water availability, and watershed management (U.S. Army Corps of Engineers, 2022). The flexibility of HEC-HMS to incorporate various hydrologic processes and data inputs, such as soil moisture accounting, snowmelt, and reservoir operations, makes it a valuable tool for both researchers and practitioners in hydrology (Sharif, Mahmood, & Nasiri, 2021). Moreover, the software's continuous development and updates ensure that it remains relevant with the latest scientific advancements and computational techniques (U.S. Army Corps of Engineers, 2022). By integrating GIS data, HEC-HMS enhances the spatial analysis capabilities, providing a more accurate representation of the watershed's physical characteristics (Maidment D. , 2019).

#### 2.2.2.1 Terrain Data

The terrain elevations from ground sites sampled at regularly spaced horizontal intervals, including the elevations of the highest and lowest points, are contained in the DEM that was created using contour lines (Gandi & Sarkar, 2016). The DEM is added to HEC-HMS as Terrain Data, and is then linked to the Basin Model. It is the main input for the GIS extension, where it is processed to automatically delineate the watershed, and create the hydrologic network of the catchment (Subbasins and reach elements). It is important to note that the DEM should be projected, and have the same coordinate system as the basin model. The Projected Coordinate System used is “Palestine_1923_Palestine_Grid”.

#### 2.2.2.2 Basin Model

A basin model allows for the physical visualization of a watershed. Automatic delineation of basins using HEC-HMS involves a systematic process facilitated by computational algorithms. Initially, digital elevation models (DEMs) are processed to identify watershed boundaries and flow directions. This step is crucial as it defines the spatial extent of the watershed under study. Subsequently, the delineated watersheds are characterized by their geometric properties such as area, perimeter, and shape indices, which provide insights into their hydrological behavior. The delineation process is often followed by parameterization, where hydrological parameters such as soil types, land use, and vegetation cover are assigned to the watershed elements. These parameters play a significant role in simulating the hydrological processes within the watershed using HEC-HMS. Once the delineation and parameterization are completed, the hydrologic model is calibrated and validated against observed hydrological data to ensure its accuracy and reliability in predicting watershed responses to various hydro-meteorological inputs. This automated approach streamlines the watershed delineation process, enabling efficient hydrological modeling and management of water resources (Maidment D. , 2019).

The following basin model is the result of the automatic delineation of the watershed using the GIS extension, it will be approved as the physical representation of Al Zeimar catchment.

**Figure 1**

*Al Zeimar Catchment Basin Model*

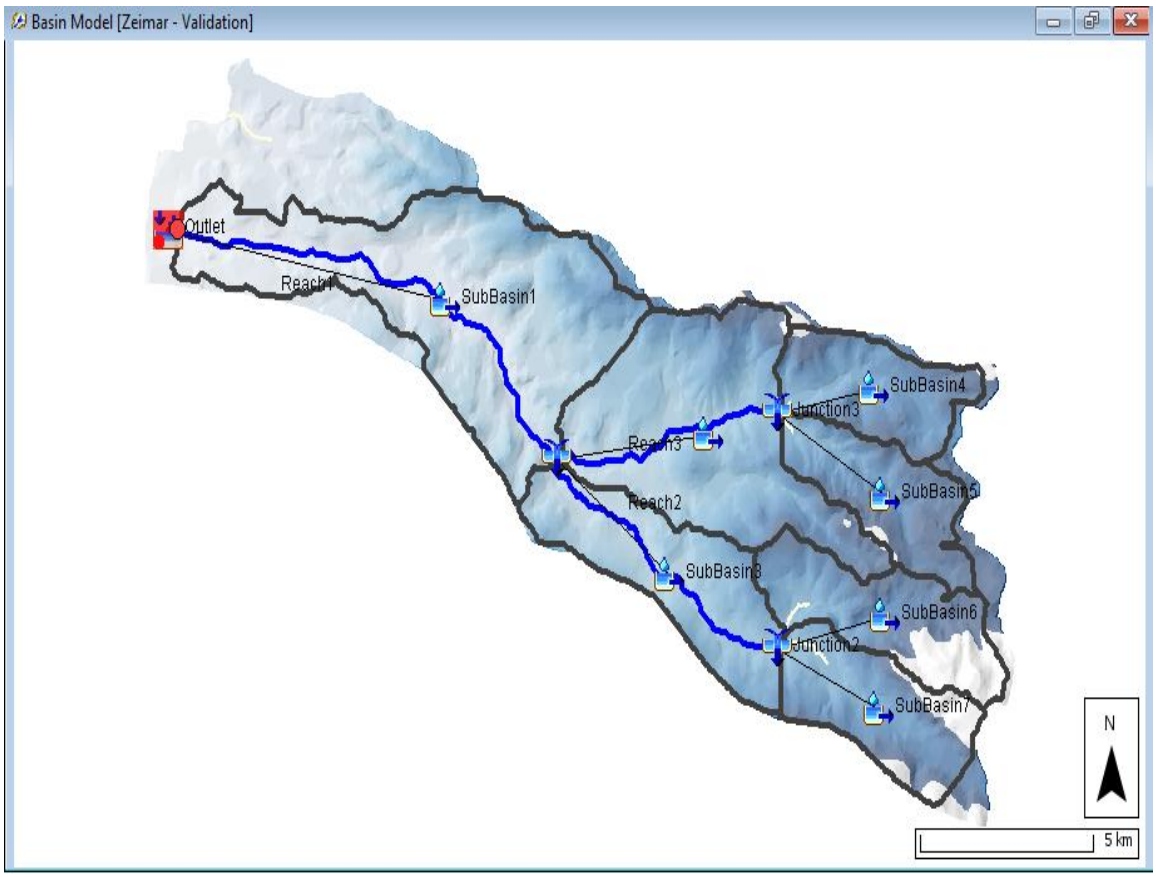


Hydrologic elements are connected together in a network to simulate runoff processes. Available elements include subbasins, reaches, junctions, and sinks (Feldman & Hydrologic Engineering Center U.S, 2022) .

**Subbasins**

It is worth considering segmenting the watershed into hydrologic units consisting of areas with consistent shapes. If achievable, these subareas ought to be around the same size, have a uniform drainage pattern, and uniform land use (Feldman & Hydrologic Engineering Center U.S, 2022). Table 1 shows the communities within each sub-basin.

**Table 1**

*Communities with each sub-basin*

| Sub-basin | Community |
|---|---|
| 1 | Bazaria, Anabta, Kfr Labad, Kfr Ruman, Ezbet Abu Khmesh, Noor Shams Camp, Bal'a, Iktaba, Shweikah, Zenaba, Tulkarem City |
| 2 | Burqa, Ramin, Masodeya, Sebastya, Naqora |
| 3 | Qusin, Beit Iba, Deir Sharaf, Beit Led |
| 4 | Beit Imrin, Nisf Jbeil |
| 5 | Ijnesenya |
| 6 | Asira Shamaliya, Zawata |
| 7 | Nablus City, Juneid, Beit Wazan, Al Ain Camp |

It is important to note that the communities within the same subbasin discharge to the same outlet (named junction in the figure 1).

Table 2 shows the physical properties of each subbasin (automatically calculated from HEC-HMS):

**Table 2**

*Physical properties of each sub-basin*

| Sub-basin | Area $km^2$ | Longest Flow Path km | Basin Slope | Drainage Density $km/km^2$ |
|---|---|---|---|---|
| Sub-Basin1 | 41.055 | 17.61 | 14.52% | 0.355 |
| Sub-Basin2 | 30.100 | 12.02 | 15.42% | 0.243 |
| Sub-Basin3 | 16.683 | 10.31 | 11.8 % | 0.535 |
| Sub-Basin4 | 10.888 | 7.25 | 17.8% | 0.048 |
| Sub-Basin5 | 10.956 | 8.48 | 17.2% | 0.078 |
| Sub-Basin6 | 13.595 | 9.90 | 19.1% | 0.130 |
| Sub-Basin7 | 12.730 | 7.94 | 21 % | 0.136 |

Table 3 shows the initial input parameters for each subbasin for the model development:

**Table 3**
*Initial input parameters for each sub-basin*

| Sub-basin | Lag Time (min) | Initial Abstraction (mm) | Curve Number |
|---|---|---|---|
| 1 | 46 | 14.32 | 78.7 |
| 2 | 33 | 14.45 | 77.85 |
| 3 | 33 | 16 | 76 |
| 4 | 21 | 17.2 | 74.7 |
| 5 | 24 | 16.93 | 75 |
| 6 | 26 | 13.5 | 79 |
| 7 | 21 | 12.7 | 80 |

It is important to note that for the curve number and initial abstraction, any AMC condition can be used, but it should be the same condition used for both parameters. (This only works for HEC-HMS)

### a. Reaches

The river or stream are conceptually presented as streams. Muskingum[1] routing method was applied to route these channels using the collected data and equations mentioned in the methodology. The Table 4 shows the initial input model parameters:

**Table 4**
*Initial input parameters for each reach*

| Reach | Length (km) | Slope | Channel Dimensions Width-Depth (m) | | Mannings' n | Muskingum K (Hr) | Muskingum X |
|---|---|---|---|---|---|---|---|
| 1 | 14.59 | 0.01028 | 6 | 2 | 0.035 | 3.12 | 0.2 |
| 2 | 8.95 | 0.01397 | 2 | 1 | 0.03 | 2.92 | 0.2 |
| 3 | 7.34 | 0.02045 | 1.3 | 1 | 0.03 | 2.40 | 0.2 |

### b. Junctions

Junctions are elements with one or more inflows and only one outflow. All the inflow is added together to produce the outflow by assuming zero storage at the junction. It is representing a river or stream confluence (Feldman & Hydrologic Engineering Center U.S, 2022). The subbasins upstream of the junction have a higher elevation, and their

[1] It is important to note that the Muskingum routing method implements full unsteady flow for open channels.

water drains into the junction by gravity. So, the junction at the end of each sub-basin is like the outlet of that subbasin, but the inlet of the sub-basin downstream of it.

**c. Sink**

The sink usually represents the lowest point of the watershed. It is the "plug" were the water sinks by gravity (Baths, 2023). The sink of the model was set at the location of the partial flume with projected coordinates of (152047,192247). It is important to note that the wadi flows beyond this point through the apartheid wall to the Yad Hana WWTP, then flows toward Netanya in historic Palestine until it discharges into the Mediterranean. Figure A.12 in Appendix A shows the partial flume at the outlet of the catchment.

#### 2.2.2.3 Time-Series Data

The HEC-HMS model requires time-series data of:[1]

1. Rainfall data for estimating basin-average rainfall.
2. Flow data, or observed discharge, which is helpful for calibrating the model.

- **Precipitation Gauge**

  There are several rainfall gauges in the catchment (mentioned in the study area section with details), but they measure daily rainfall. The model is event based, so data with a small-time interval is needed. The rainfall data used was obtained from the Qarni Shomron Station (IMS, 2023), which almost lies in the middle of the catchment, because it is the only rain station in the catchment that contains 10-minute rainfall data. Since only one precipitation gauge is used, the model considers that rainfall from this gauge is distributed uniformly all over the catchment. The storm that was used for Run 1 of the model started on 11 February 2020 at 22:00 and ended on 12 February 2020 at 09:00. It resulted in 11 mm of rain over the 11-hour period. The hyetograph in Figure A.13 was drawn by HEC-HMS for Storm 1. It shows the temporal distribution of rainfall. It can be noted that from 22:00 to 02:00, the rain was light, but after 02:00, the rain started to increase at reached its highest amount at 05:00 almost, then started to decrease and ended at 09:00.

[1] Time-series data are stored in the project as a gage.

- **Discharge Gauge**

  The data for the discharge gauge was obtained from the partial flume. As mentioned earlier, in winter, rainwater is mixed with treated wastewater in the wadis, so the partial flume reads both. The following methodology was used to quantify the discharge from rainwater only:

  1. Collection of the 24-hour readings of the partial flume for a dry winter day Qt (This represents amounts of treated wastewater only that the partial flume read)
  2. Calculate their sum, $Q_D$
  3. Plot $Q_t$ / $Q_D$ vs. Time
  4. Check that $\sum \frac{Qt}{QD} = 1$
  5. The plot represents the 24-hour wastewater flow pattern at the partial flume
  6. To quantify discharge from rainfall, on a rainy day, determine the amount of treated wastewater discharged from the Nablus Western WWTP ($Q_{ww}$)
  7. Multiply $Q_{ww}$ with the wastewater flow daily pattern
  8. The resulting $Q_{wwg}$ is the wastewater amounts at the partial flume on the day of the event
  9. $Q_R = Q_T - Q_{wwg}$, where $Q_R$ is the runoff from effective rainfall

Steps 1-5 were applied on 15 February 2020 (This day has zero rainfall), and the graph in Appendix A is the wastewater flow pattern at the partial flume. When treated wastewater is discharged from Western Nablus WWTP into the wadis, it does not reach the partial flume at the end of the catchment in the same amount as part of it evaporates and some infiltrates through the wadis bed. The pattern above is used to temporally quantify the 24-hr amount of treated wastewater that reaches the partial flume from the WWTP. For example, on 15 January of 2022, the treatment plant reported that 11,000 $m^3$ was discharged into the wadi. This number is multiplied by Qt/QD for 24-hours to obtain the amount that reached the outlet. For instance, at 23:20, 880 $m^3$ reached the outlet (0.08x11,000 = 880 $m^3$).

The runoff "Runoff 1" resulting from Storm 1 starts at 12Feb2020 at 00:30 and ends at 12Feb2020 at 20:00. Storm 1 started at 11Feb2020 at 22:00, but the runoff from the storm started to reach the outlet at 00:30 on 12Feb2020, after two and a half hours of the storm, which means that the catchments' lag time is approximately two and a half hours. The

runoff hydrograph of Storm 1 is shown in Figure A.14 in Appendix A, this figure was drawn by HEC-HMS. The data was obtained from the partial flume, and wastewater flow was quantified and removed. The peak flow is 0.5 $m^3/s$ and occurs at 06:00. It is noticeable that the hydrograph has two peaks. Two peaks appear on a double peak hydrograph in response to a distinct rainfall pulse. The first peak, which represents a quick catchment response to precipitation, happens simultaneously with or soon after the precipitation begins. Usually, the delayed peak begins when the first peak is receding and the precipitation has stopped. In urban catchments, double peak hydrographs can arise for a variety of reasons. Direct surface runoff on impermeable land cover frequently causes the initial peak, and slower subsurface flow is responsible for the delayed peak (Martinez-Carreras, et al., 2016). The double peak can be explained in the Zeimar stream because in the Anabta section, 200 meters of the channel is built up concrete. In addition, the section ahead of the partial flume is made up of concrete, this facilitates the flow of water and thus it reaches faster to the outlet. Figure A.15 in Appendix A shows the built-up part section in Anabta.

#### 2.2.2.4 Meteorological Models

One of a HEC-HMS hydrologic model primary components is a meteorologic model. Preparing meteorologic border conditions for sub-basins is the main goal (Feldman & Hydrologic Engineering Center U.S, 2022). Based on the used event, it is assumed that there is one precipitation gauge uniformly covering the catchment.

#### 2.2.2.5 Control Specifications

Despite having little in terms of parameter data, control specifications are a key part of the model. Their main function is to regulate the start and stop times of simulations as well as the time intervals that are used (Feldman & Hydrologic Engineering Center U.S, 2022).

### 2.2.3 Model Calibration and Validation

Hydrological models are the mathematical models having some unknown coefficients known as parameters. The process of estimating those parameters from previous input-output records is known as model calibration. Model validation is evaluating the calibrated model's performance across the historical record section that was not used for

the calibration. Calibration is typically done via trial and error. Different validation criteria are utilized for the model validation, and they are constructed based on the output records that are computed and observed (Lohani, Rainfall - Runoff Analysis and Modeling, 2016).

Basically, four sources of uncertainty occur in deterministic simulation. The differences between recorded and simulated output result from:

1. **Error Source 1**: Errors in the input data that are either random or systematic, such as temperature, precipitation, or evapotranspiration, and which are utilized to depict the catchment's input conditions in both space and time.
2. **Error Source 2:** Errors in the recorded output data that are either random or systematic, such as discharge or water level data that are compared to the output of the simulation.
3. **Error Source 3:** Errors due to non-optional parameter values, e.g., rain gage location (latitude and longitude) and the rain gage data file.
4. **Error Source 4:** Errors due to incomplete or biased model structure. e.g., neglecting groundwater flow, and not considering all sources of runoff.

As a result, only error source 3 is reduced during the calibration process, whereas all four error sources are to blame for the discrepancy between the simulated and recorded output. As "background noise," the measurement errors and error source 2 provided a minimal degree of disagreement below which changing any more parameters or tweaking the model won't make the findings better. The next step in the calibration process is to minimize error source 3 until it becomes negligible in comparison to data error sources 1 and 2 (Lohani, Rainfall - Runoff Analysis and Modeling, 2016). An accuracy criterion can be used to compare the measured and simulated outputs during the calibration process. This makes it possible to determine the ideal parameter values and to get an objective evaluation of the goodness of fit linked with each set of parameters. (Lohani, 2016) The Nash-Sutcliffe model efficiency coefficient (NSE) is preferably used to assess the efficiency of hydrological models (Ikenberry, n.d.).

$$E = \frac{\sum(O_i - \bar{O})^2 - \sum(M_i - O_i)^2}{\sum(O_i - \bar{O})^2} \qquad (16)$$

O = Observed Values ($m^3/s$)

$\bar{O}$ = Average of Observed Values ($m^3/s$)

M = Modeled Values ($m^3/s$)

The maximum value of *E* is 1. A value of zero indicates that the model is only as good as using the mean of the observations. *E* can be less than zero (Ladson, 2008). The following table identifies the classification (Goodness) of the model depending on the value of E for the calibration and validation processes.

**Table 5**

*Classification of model performance according to E*

| Classification | E (Calibration) | E (Validation) |
|---|---|---|
| Excellent | $E \geq 0.93$ | $E \geq 0.93$ |
| Good | $0.8 \leq E < 0.93$ | $0.8 \leq E < 0.93$ |
| Satisfactory | $0.7 \leq E < 0.8$ | $0.6 \leq E < 0.8$ |
| Passable | $0.6 \leq E < 0.7$ | $0.3 \leq E < 0.6$ |
| Poor | $E < 0.6$ | $E < 0.3$ |

Another calibration parameter is percent bias. Percent bias (PBIAS) calculates how likely it is on average for the simulated values to differ from the observed values. PBIAS should ideally be at 0.0, with low magnification values denoting precise model simulation. Overestimation bias is indicated by positive numbers, whereas underestimating bias in the model is indicated by negative values (Bigiarini, PBIAS HydroGOF, 2010).

$$PBIAS = 100 \frac{\sum_{i=1}^{N}(S_i - O_i)}{\sum_{i-1}^{N} O_i} \quad (17)$$

S= Simulated Values ($m^3/s$)

O = Observed Values ($m^3/s$)

### 2.2.4 Projection of EPI to Simulate Climate Change

#### 2.2.4.1 Extreme Precipitation Indices of the Study Area

Table 6 shows indices for the period from 1997-2022 for the Nablus station. (The data was obtained from manually processing rainfall data from (Palestinian Meteorological Department, 2024) using excel).

**Table 6**
*EPI for Nablus for 1997-2022*

| Parameter | Precipitation (mm) |
|---|---|
| SDII | 12.5 |
| Rx1 day | 123 |
| 99p | 32.2 |
| 90p | 16.4 |

Table 6 shows that the average precipitation on rainy days for the period between 1997-2022 is about 12.5 mm. The maximum daily rainfall that occurred during this period was 123 mm, and this occurred in 2013 in storm Alexa. When projecting the outputs of the study done by (Hochman, Mercogliano, Alpert, Saaroni, & Bucchignani, 2018) on the Nablus station EPI's, the extreme EPIs of the study area in the period from 2041-2070, according to the output of the climate projections become:

**Table 7**
*EPI for Nablus for 2041-2070*

| Parameter | Precipitation (mm) |
|---|---|
| SDII | 11.5 |
| Rx1 day | 135 |
| 99p | 46.2 |
| 90p | 13.4 |

The mean daily rainfall during rainy days, decreased by 1 mm, to become 11.5 mm/day. This supports the theory that the total amounts of rainfall will decrease in the years 2041-2070. As for the maximum amount of daily rainfall over the years 2041-2070, it is 135 mm/day which also supports the claims of (Assaf, Paola, Pinhas, & Hadas, 2018) that the chances of flash flood will increase.

#### 2.2.4.2 Frequency Analysis of Nablus Station Meteorological Data

Olofintoye et al. (2009) stated that even though the characteristics of precipitation are unpredictable and change over time, it is feasible to predict the amount of rainfall with extreme precision for various durations by employing a certain probability distribution. As a result, statistical frequency analysis of the maximum rainfall records completes the estimation of heavy rainfall. Since the frequency of extreme occurrences affects flood

control systems' functioning and design, it is imperative to evaluate the statistics of extreme precipitation events (Doan, et al., 2015). HEC-SSP[1] is a software developed by the US Army Corps of Engineers, it stands for Hydrologic Engineering Center's (HEC) Statistical Software Package (HEC-SSP). This software allows users to perform statistical analyses of hydrologic data. It was used to conduct the frequency analysis of the maximum daily rainfall data for the years 1997-2022 Table B.9 in Appendix B (Data retrieved from Palestinian Meteorological Department (2024)) of Nablus station. The Chi-Square was used to determine the best distribution that represents the maximum daily rainfall data. The chi-square ($\chi^2$) statistic is a tool used to assess how well a model fits real-world observations. It calculates the discrepancy between the actual and predicted frequencies of a given set of variables or occurrences (Hayes, 2023). The smaller the Chi-square value, the better the distribution fits the data. The normal distribution was the best distribution to fit the maximum rainfall data of Nablus for the years 1997-2022. The fitted distribution has been used to calculate the size of an event which correlates to a return period of 25 years, then the increase in the maximum daily precipitation from Table 7 was added.

Figure 2 shows the cumulative distribution function – plotting position of the maximum rainfall data, and the normal distribution curve.

[1] https://www.hec.usace.army.mil/software/hec-ssp/download.aspx

**Figure 2**

*CDF of maximum daily rainfall data of Nablus Station*

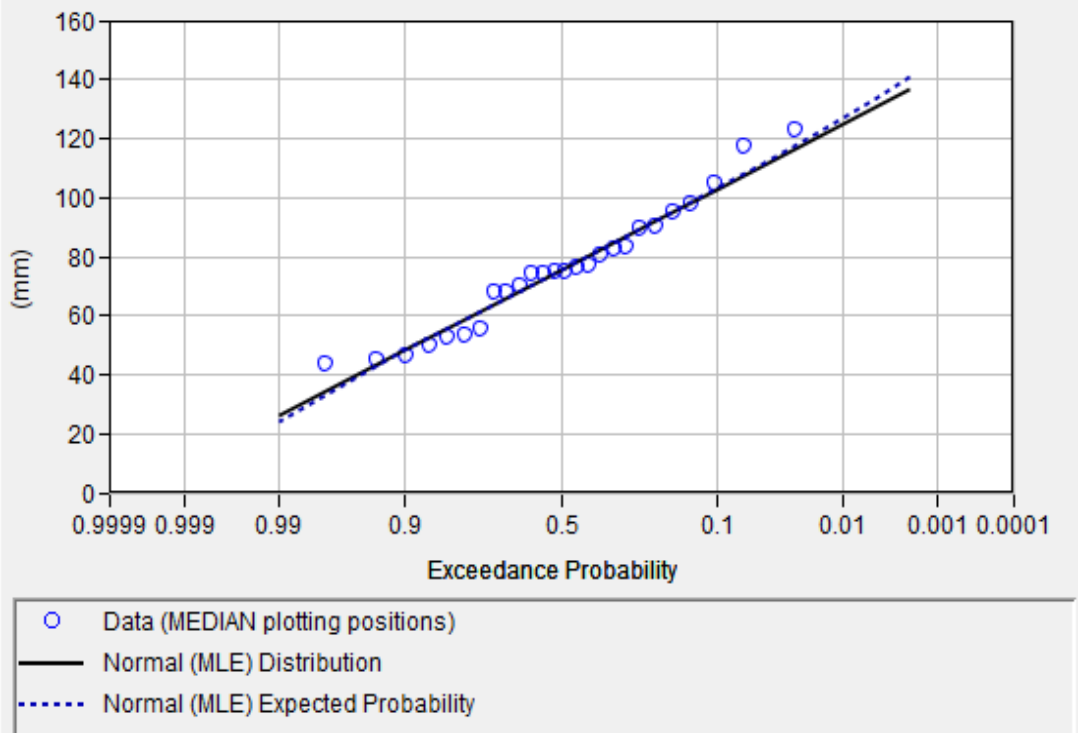


According to (WSDOT, 2023), culverts are designed for the 25- and 100-years flow events. In this study, the 25 years flow event was used for the design because it is within the climate change projections period (2041-2070). The probability of exceedance of the 25-year maximum daily rainfall event is 1/25 = 0.04 from Figure 2, the expected maximum daily rainfall after 25 years is 113 mm. According to the climate projections in Table 7 the maximum daily precipitation increase by 12 mm, which makes the maximum daily rainfall in that period 125 mm.

### 2.2.4.3 Meteorological Climate Change Scenario Input for the Model

The maximum daily rainfall from the previous section is 125 mm. To be able to use this as an input for the HEC-HMS model, it should be converted into a 10-min interval event. To achieve this, the 2013 Alexa hyetograph distribution was used to simulate a synthetic 24-hour, 5-min interval storm. Figure A.16 in Appendix A shows the hyetograph of Alexa storm, it was extracted from Weather Underground (n.d.) which is a commercial weather service that provides weather data online.

Figure 3 shows the hyetograph of a synthetic storm with the same temporal distribution of rainfall as Alexa, which was obtained using through obtaining the ratio of each rainfall

pulse of each interval to the total amount of rainfall for Alexa, then multiplying this ratio by 125 mm for each rainfall pulse of the synthetic storm.

**Figure 3**

*Hyetograph of the synthetic storm*

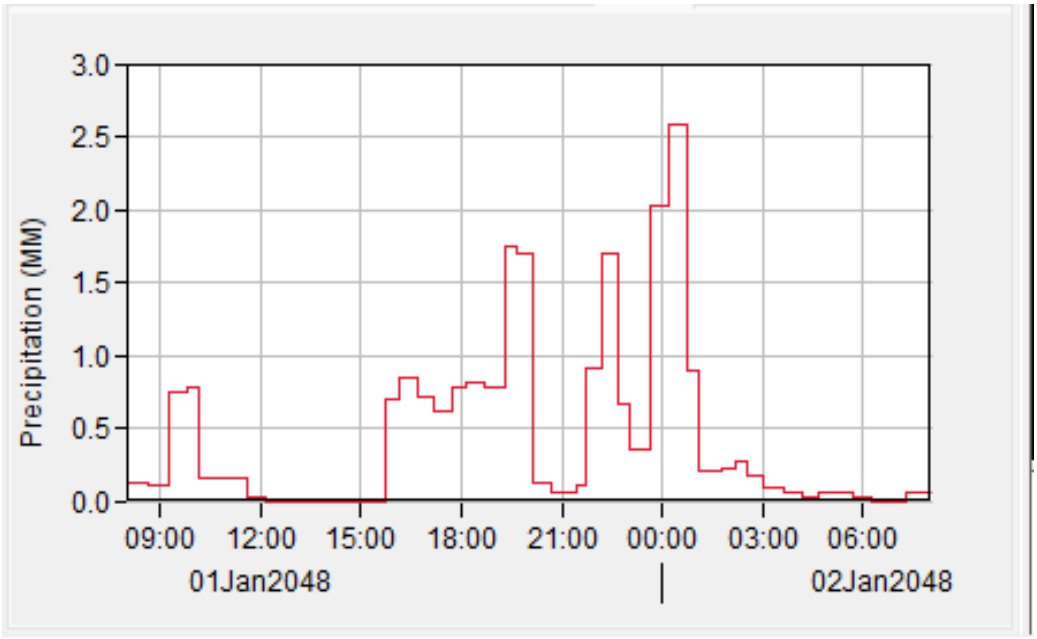


The storm starts at 08:00 am on 01Jan2048, and ends at 08:00 of 02Jan2048. From its start at 08:00 until 12:00, it rains and peaks its first peak at almost 10:00 am. From 12:00 pm until 16:00, there is no rain, then it quickly begins to rain and peaks it's second peak around 20:00, it decreases for a little while, and then starts to rain at 21:30, to peak it's third peak around 22:30, and then peaks again at 01:30, then starts to decrease gradually and end. It is important to note that the last two peaks are very dangerous rainfall pulses, because they endure a large amount of rain in a small period of time, and this is what causes the disastrous floods and corresponding hazards.

### 2.2.5 Assessment of Anabta's Culverts

#### 2.2.5.1 Description of Anabta's Culvert System

Wadi Al Zeimar is the main wadi that runs in Anabta. It contains 13 culverts from the Bizzariya junction extending to the west of the town. Figure A.17 in Appendix A shows the aerial view, from the previous study conducted by Aqua Consulting Group (AQUA Consulting Center, 2013), shows the distribution of the culverts over the wadi. The

existing culvers are made up of concrete, and most of them are rectangular. The cross-sectional area ranges from 9-18 $m^2$.

There are several houses close to the culverts, which makes them at risk in case of any flooding. The main culvert that was redesigned is culvert No. 1 in the aerial photo Figure A.17. It lays under Al Hejaz Gas Station. It is rectangular, with a span of 2 meters, and a height of 2 m, and has 2 barrels. Figure A.18 shows the culvert, and it is noticed that the wadi is very dirty, and as mentioned earlier, the uncontrolled dumping of garbage in the wadi reduces the capacity of the culverts and leads to environmental and health negative consequences. It is also noticeable that the culvert is close to the street and above it is a residential building and a parking lot.

#### 2.2.5.2 HY-8 Culvert Hydraulic Analysis Program

The program that was used to redesign the culvert is HY-8[1]. It is developed by the US Department of Transportation – Federal Highway Administration. HY-8 uses several key elements to automate culvert hydraulic simulations, simplifying culvert analysis and design. It assesses the culverts' effectiveness and determines whether or not the road overtops (Smemoe, 2022).

Culvert No.1 was redesigned based on the peak flow at Anabta resulting from the climate change scenario (Run 4). The culverts' inlet elevation, outlet elevation and the roadway crest are respectively 166.6 m,166.5 m, 169.19m amsl. Overtopping of the roadway occurs when the elevation of water in the culvert exceeds 169.19 m. So, the proper design for the culvert considers that the water level must not exceed the roadway level, in addition, backflow of water must not occur. HY-8 automatically designs within these measures.

[1] https://www.fhwa.dot.gov/engineering/hydraulics/software/hy8/

# Chapter Three

# Results

## 3.1 Simulation Runs

The main way to compute the results is through simulation runs. One basin model, one meteorological model, and one set of control requirements make up each run (Feldman & Hydrologic Engineering Center U.S, 2022). Run 1 is made up of Al Zeimar catchment Model, Storm 1, and Runoff 1. Run 2 is used for calibration while Run 3 is for validation. Run 4 is used to simulate the future shift in climate.

- For Run 1 the peak discharge at the outlet occurred at 08:30, with a value of 0.5 $m^3/s$**.** The efficiency parameter (E) was 0.343, and the percent bias (PBias) was -24.75%. E is 0.343 so the models' performance is passable.

The model produced the same peak discharge as the observed data, but the difference is in the time of occurrence The hydrograph at the sink (outlet) is shown in Figure 4 below.

**Figure 4**

*Hydrograph of Run 1*

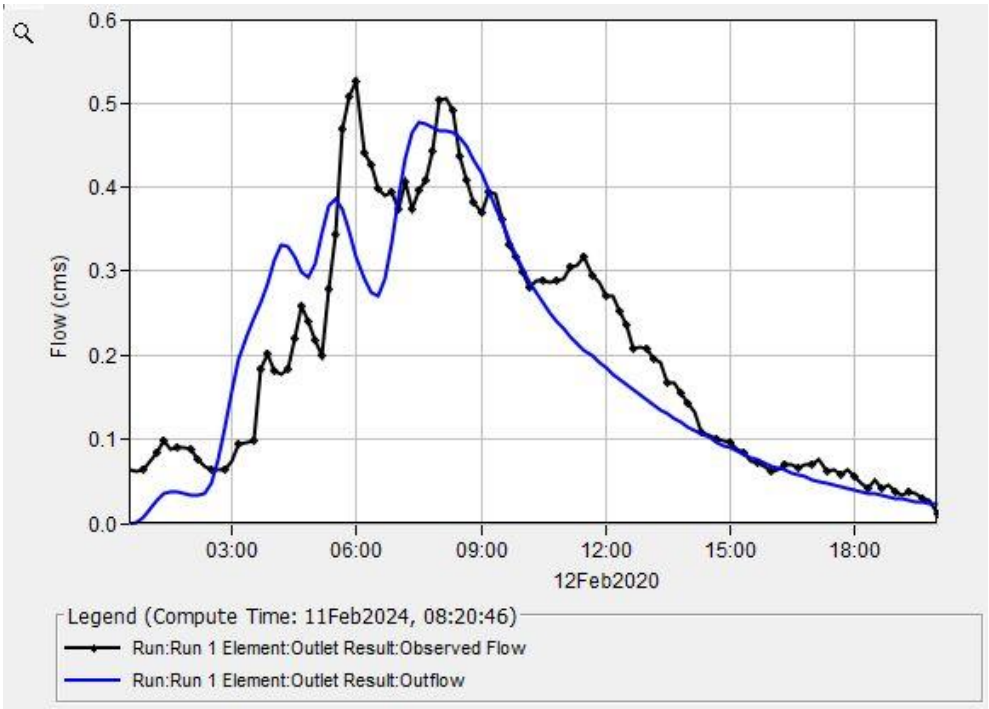

The following points discuss the behaviour of both observed and simulated hydrographs of Figure 4:

2. At the first minute of the storm (time 00:00), the observed hydrograph had a reading of 0.18 $m^3/s$, this reading is probably unquantified treated wastewater, while the model had a reading of zero. It is impossible for the model to give an instant reading because there are a number of losses. This error is due to error source 4 listed previously, where the model is uncomplete because HEC-HMS doesn't have the option of defining sources of runoff other than storm water, and the wadi in reality has treated wastewater flowing in it.
3. At 00:30, both hydrographs have the same behavior, but the modeled hydrograph underestimates the runoff, until at 02:20, both hydrographs intersect, and the simulated over estimates runoff, until 09:20 where they intersect again.
4. In the observed hydrograph, the first peak occurred at 06:00 and the second occurred at 08:10, whereas in the simulated hydrograph, the first peak occurred at 07:00 and the second at 08:20, which shows a delay in the occurring of peaks and a slight underestimation of their values. The peak flow timing discrepancy occurs because the simulated hydrograph is generated using mathematical models, which makes the hydrograph sensitive to the model parameters, especially the lag time, where any under or over estimation in the lag time affects the time of the peak. Additionally, the precipitation data (limited stations that do not capture all sub catchments) and the assumption of uniform rainfall distribution all over the catchment (that may not perfectly match the reality) also cause the discrepancy.
5. The real flow data has more pronounced peaks, suggesting it captures more detailed variations in flow. The modeled hydrograph is smoother and less variable. This smoothness might result from the simplifications in the model that don't capture the steep slopes, valleys and impermeable surfaces which affect the flow.

### 3.2 Model Calibration

In order to reduce the differences between both hydrographs (observed and simulated in Figure 4) to obtain reliable real results, calibration was manually done to the model parameters using the trial-and-error method. The peak discharge of 0.5 $m^3/s$ occurred at 08:30, the NSE coefficient increased to 0.863, and percent bias decreased to 0.58%. The following is the
hydrograph of Run 2 at the sink of the catchment.

**Figure 5**
*Hydrograph of Run 2*

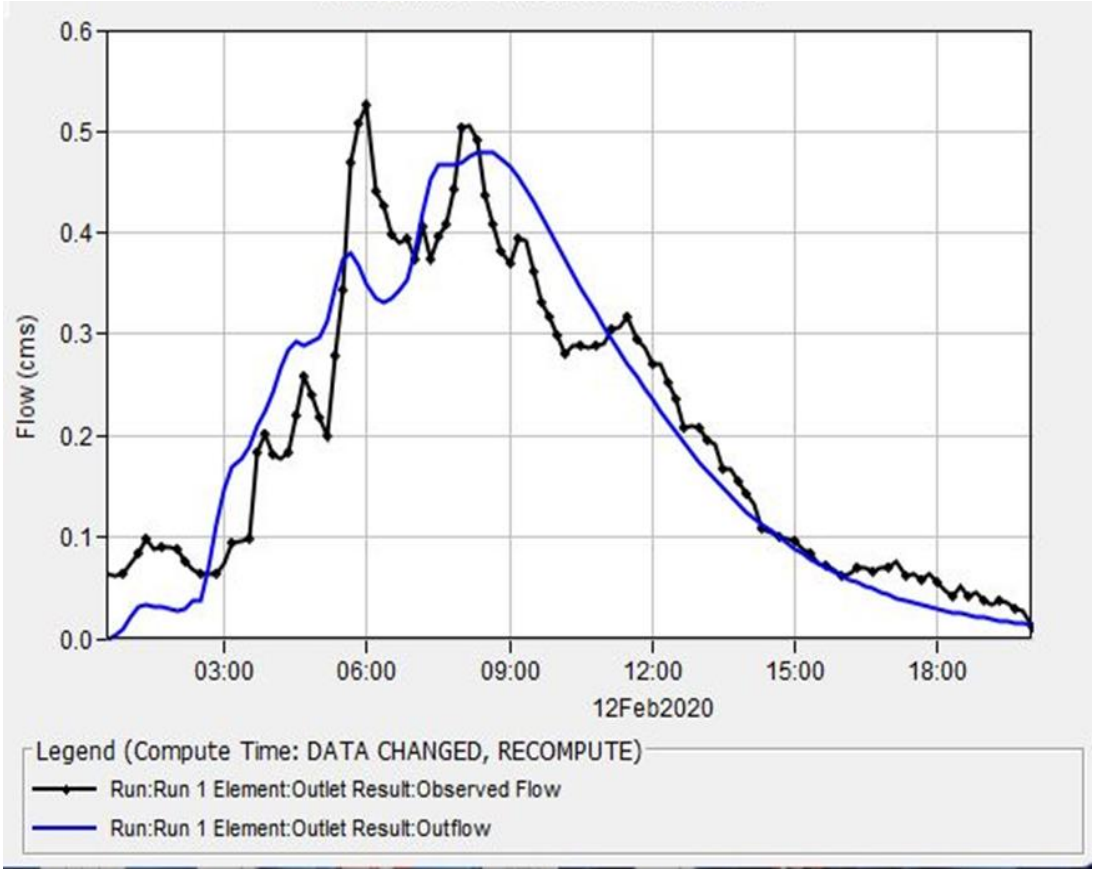


By visually inspecting the hydrograph, the following comments can be concluded:

1. Both hydrographs are similar in shape and magnitude. Both almost give a peak discharge of 0.5 $m^3/s$, the difference is the time of occurrence of it. In the real storm, the peak occurred at 06:00, but in the model it occurred at 08:30.
2. It is important to mention that the calibrated simulated hydrograph is smoother than the observed one. The simulation process involves averaging out short-term

flocculation, which means that rapid and sudden changes in the flow rate are smoothed over. The smoothed hydrograph is useful in long-term planning and infrastructure design, where it provides insights into overall trends without being overly influenced by short-term variations.

Tables 8 ,9, and 10 show the differences between initial and calibrated parameters for each input parameter:

- Transform – SCS UH

**Table 8**

*Initial and Calibrated Lag Time*

| Lag Time (min) | Initial | Calibrated |
|---|---|---|
| Sub-basin 1 | 46 | 40 |
| Subbasin 2 | 33 | 29 |
| Subbasin 3 | 33 | 20 |
| Subbasin 4 | 21 | 20 |
| Subbasin 5 | 24 | 15 |
| Subbasin 6 | 26 | 15 |
| Subbasin 7 | 21 | 15 |

The calibrated lag times are generally lower than the initial lag times. This indicates that the calibration process has identified a need for faster response times in the model, likely to better match observed data.

- Loss – SCS CN

**Table 9**

*Initial and Calibrated SCS CN Parameters*

| Subbasin | Initial Abstraction | | CN | |
|---|---|---|---|---|
| | Initial | Calibrated | Initial | Calibrated |
| 1 | 14.32 | 12 | 78.7 | 76 |
| 2 | 14.45 | 13.14 | 77.85 | 78 |
| 3 | 16 | 13.2 | 76 | 76 |
| 4 | 17.2 | 11.55 | 74.7 | 70 |
| 5 | 16.93 | 11.9 | 75 | 75 |
| 6 | 13.5 | 14 | 79 | 79 |
| 7 | 12.7 | 12.9 | 80 | 80 |

The CN values show minor adjustments, with some sub-basins experiencing slight increases or decreases. This indicates that the initial estimates were relatively close to the observed values, requiring only fine-tuning

- Routing -Muskingum

**Table 10**

*Initial and Calibrated Muskingum Parameters*

| Reach | K (hr) | | X | |
|---|---|---|---|---|
| | Initial | Calibrated | Initial | Calibrated |
| 1 | 3.11 | 3.6 | 0.25 | 0.3 |
| 2 | 2.92 | 2.4 | 0.25 | 0.3 |
| 3 | 2.39 | 2.3 | 0.25 | 0.38 |

The K values show both increases and decreases across different sub-basins. This suggests that the calibration process identified a need for varied adjustments to better simulate the flood wave travel time through the river reach. The adjustments in K values improved the model's ability to simulate the timing and attenuation of flood waves more accurately.

### 3.3 3.3 Model Validation

The model needs to be evaluated to help make sure it can accurately replicate hydrologic processes under various settings. Comparing the model's output with observable data from a time period other than the calibration period is a common step in the validation process (Siegfried & Marti, 2021).The storm used for validation “Storm 2” was extracted from (IMS, 2023). It started on 20$^{th}$ March of 2020 at 14:40, and ended at 15:50 at the same day. It resulted in 1.4 mm on rainfall. Figures 6 and 7 show the hyetograph and hydrograph of Storm 2.

**Figure 6**

*Hyetograph of Storm 2*

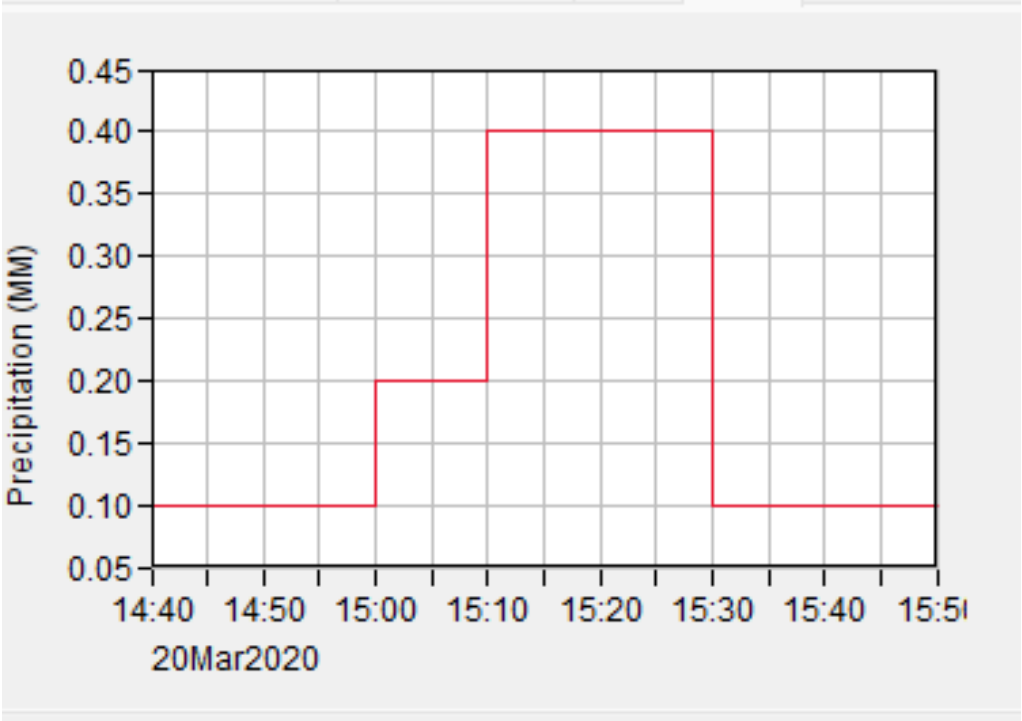


**Figure 7**

*Hydrograph of storm 2*

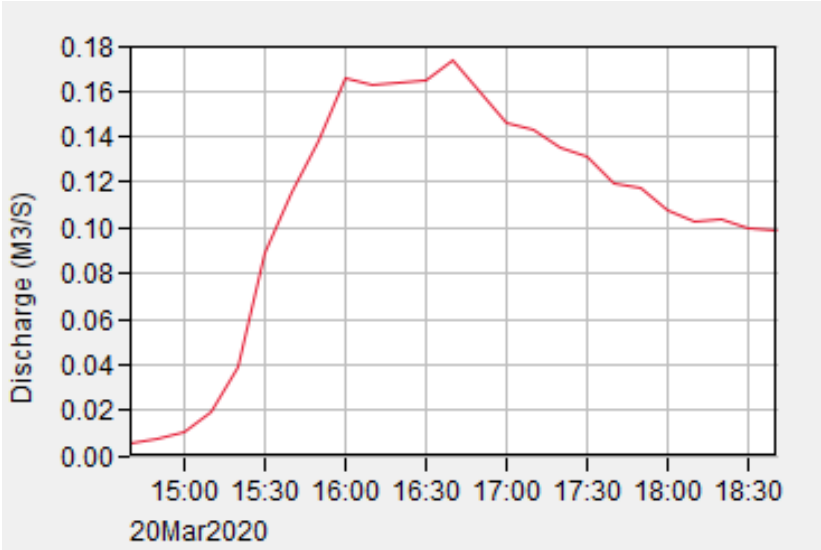


The key observations of the previous hydrograph are:

1. At approximately 16:30, the hydrograph reached its peak discharge of 0.19 $m^3/s$
2. The sharp increase in discharge occurred between 15:00 and 16:30. Within this hour and a half, the flow escalated rapidly, then started to gradually decrease.

The peak discharge at the outlet of the catchment resulting from Run 3 that simulated the previous storm is 0.2 $m^3/s$. It occurred at 16:10, and the Nasch-Sutcliff coefficient is 0.777, and PBIAS is 6.56%. The models' performance is satisfying, and the amount and time of peak are very close to the real hydrograph. Figure 8 shows the hydrograph of Run 3.

**Figure 8**

*Hydrograph of Run 3*

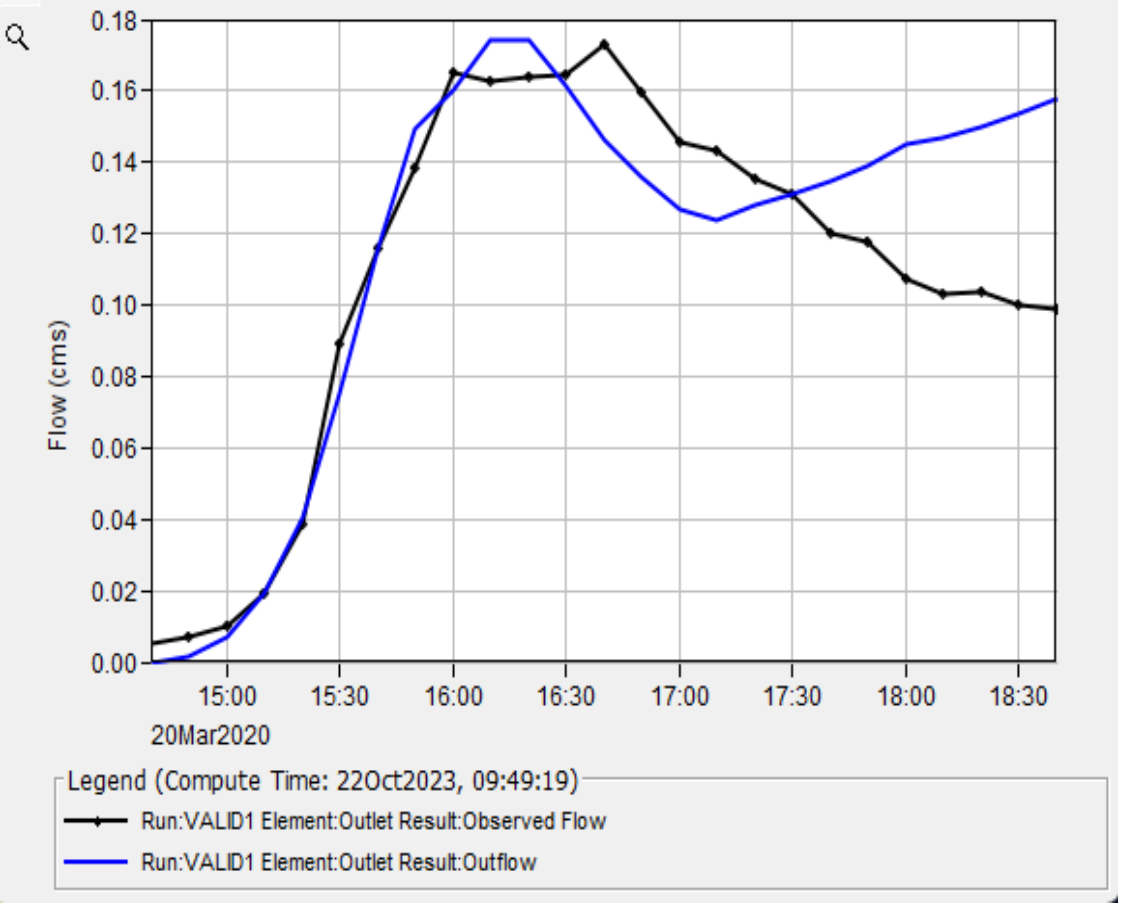


The model successfully captured the overall trend including the peak discharge. However, the initial rise is steeper in the simulated hydrograph, and the recession limb shows some deviation.

### 3.4 Climate Change Scenario Run

The synthetic storm used for Run 4 is mentioned in section 2.2.4.3. Figure 9 shows the hydrograph of the run in Anabta.

**Figure 9**

*Hydrograph of Run 4*

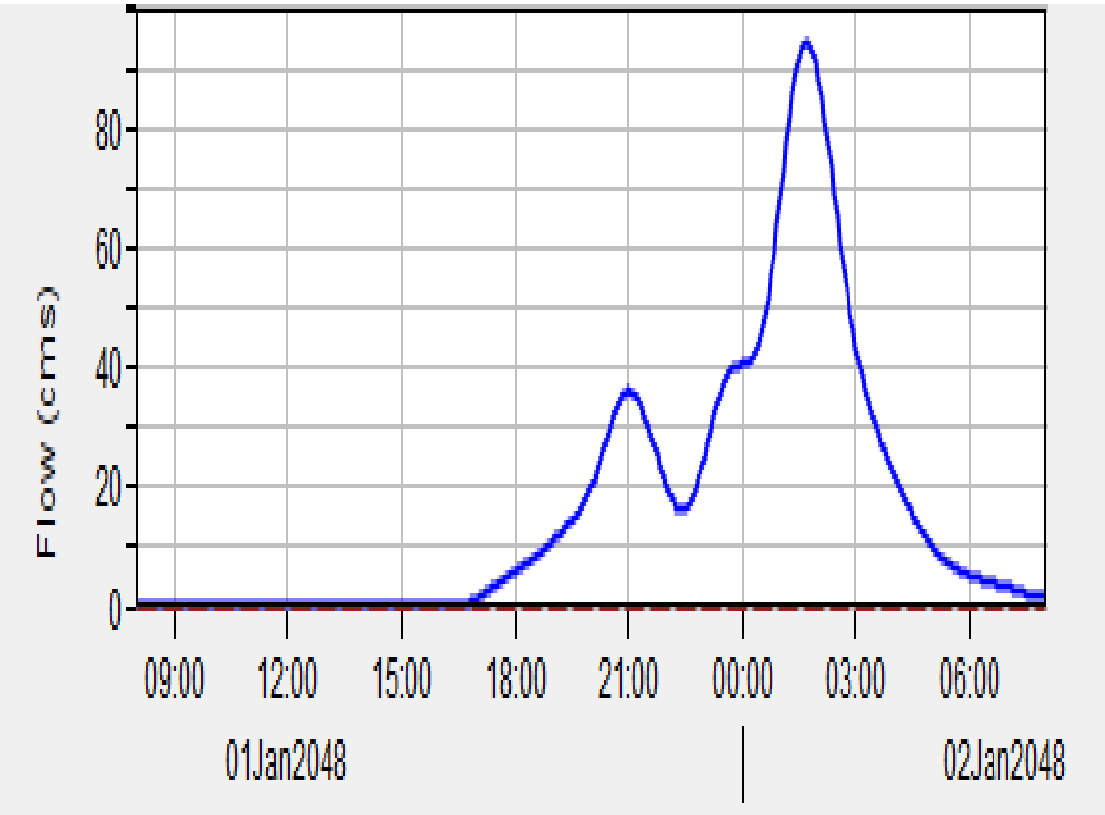


The flow starts in Anabta at almost 17:00 on 01 Jan., this is compatible with the hyetograph of the storm, where there is a small rainfall pulse at the beginning of the storm, then a bigger rainfall pulse occurs at 16:00 on 01 Jan., leading the runoff to start in Anabta.

The hydrograph has two peaks, and this behavior is similar to the behavior at the outlet of the catchment. The first peak occurs at 21:00 on 01 Jan, and the second peak occurs at 01:40 on 02 Jan. It is important to note that the peak of 92 $m^3/s$ is a very high flow value. It can be noted that the huge peak discharge is at Sub-basin 1, Reach 1, and the outlet. It occurred after the last two rainfall pulses mentioned earlier in section 2.2.4.3, and this supports the theory that rain pulses with high intensities (high precipitation over small time periods) are what cause flash floods.

### 3.5 Culvert No.1 Redesign

The peak flow rate (92 $m^3/s$) from Run 4 was used to redesign culvert No. 1 using HY-8. If this flow rate occurs with the culverts' current dimensions, it can drain only 24 $m^3/s$. Where the head water elevation will reach 172.3 m amsl, which means that 3 meters of water will overtop to the road, and will cause catastrophic damage. To prevent this from happening, the culvert was redesigned using HY-8 as follows:

- The outlet should be excavated to 166.2 m level.
- The span of each opening should increase to 3 m.
- The rise of each opening should increase to 2.5 m.
- Two additional barrels are needed.

The current area of the culvert is almost 10 $m^2$, with the new design, it should be increased to 30 $m^2$. It is important to note that the culvert cannot be enlarged this much because there are buildings on both sides, so this solution is not feasible nor applicable. Figure 10 shows a side view of the culvert.

**Figure 10**

*Side View of the Culvert*

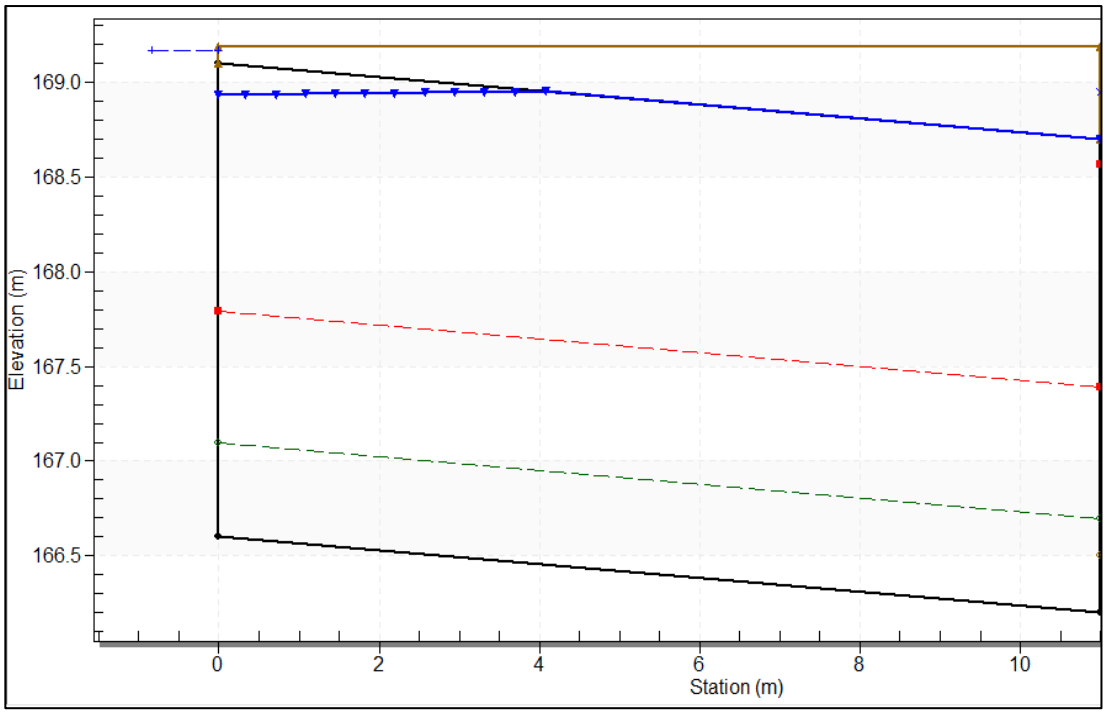


- Figure 10 shows the elevations of the inlet, outlet, and roadway. The blue line represents the level of water flowing in the culvert during the 92 $m^3/s$ peak flow rate. In the first 4 meters of the culvert, the flow level will be 168.9 m amsl, then it will flow fully with the culverts' slope. This means that with the proposed design, the culvert can handle an extreme flow rate of 92 $m^3/s$ without any flooding of water. It is important to note that this design in not applicable nor feasible, because there are houses and buildings and other elements around the culvert on both sides. Thus, other solutions should be proposed rather than enlarging culverts. Other solutions include:

- Flood mapping and zoning
- Using green infrastructure
- Detention Basins
- Channelization and river restoration

# Chapter Four

# Conclusions, Limitations and Recommendations

## 4.1 Conclusions

Even though climate change is not the most pressing issue for the people in the Palestinian Territories, the climate risks are significant and will affect current and future development challenges. The main objective of this study is to develop a rainfall-runoff model for the Al-Zeimar catchment, in order to be able to simulate and analyze the effects of climate change on the hydrology of the catchment, especially in the Anabta area, that witnessed catastrophic flooding in 2013. Data was collected, and then processed to build the HEC-HMS model. Then the future shifts in climate were projected on the study area, and used to assess the hydrological situation by testing the ability of a culvert at the entrance of Anabta to handle a 25-year storm, and it failed. A new design of the culvert was proposed using HY-8. In light of the previous steps, the following are the conclusions:

1. The HEC-HMS model performed well in simulating the impact of average occurring rainfall events, and this is reflected in the calibration and validation runs. It is important to note that this model is the first model of the area which is based on real run off data.
2. Due to the future climate shifts, the culvert at the entrance of Anabta failed to handle the 25-year extreme storm. This reflects true flood danger in the area, because Anabta has smaller and older culverts.

## 4.2 Limitations

The following are the limitations of the study:

1. Data availability and reliability is a central point, especially in model building. Unfortunately, precise and reliable data are not available. For example, for precipitation data, the main available data is the daily and annual rainfall, and for models, smaller intervals are needed. There are a lot of data gaps, and a lot of uncollected data. All this makes the development of optimal solutions harder.
2. There is no flow data measuring devices in the catchment. There is a partial flume that was installed at 2020 at the outlet, but its main use is to quantify treated

wastewater that flows all year in the wadis downstream of the treatment plant. It measures up to 90 cm of combined water, and this means small amounts of flow. This was a major limitation while calibrating and validating the model.

3. There is no geodatabase for the rainfall and flow data. Data is disorganized and scattered and this made the collection of data take a very long time.

### 4.3 Recommendations

Regarding the research methods and ability to improve model results, the following recommendations can be taken into consideration:

- Rainfall measuring devices for small intervals should be installed. Where the high density of rainfall gauges allows to capture localized variations in rainfall properties, therefore, enhance the accuracy and reliability of all the hydrologic studies In addition, it helps in investigating the response of the sub-catchments to different events. It is recommended that the rain gauges are installed downstream of potential flood-prone areas.

- Rainfall and flow data within catchments should be systematically collected, cataloged, and maintained within a centralized database. This serves as a fundamental resource for hydrological analysis, watershed management, and informed decision-making in water resource planning and flood mitigation efforts. By systematically documenting rainfall patterns and streamflow dynamics across catchment areas, this database facilitates a deeper understanding of hydrological processes, enabling researchers, policymakers, and water resource managers to identify potential risks. Moreover, the availability of historical data allows for the calibration and validation of hydrological models, enhancing their accuracy and reliability in predicting future scenarios and assessing the impacts of climate change on watershed hydrology.
- Further study of the impacts of climate change on Anabtas culverts should be conducted.

# List of Abbreviations

| Abbreviation | Meaning |
|---|---|
| AMC | Antecedent Moisture Content |
| $C^o$ | Degrees Celsius |
| CN | Curve Number |
| COSMO-CLM | Climate Limited-Area Modeling Community |
| DEM | Digital Elevation Model |
| EPI | Extreme Precipitation Indices |
| GIS | Geographic Information System |
| GPS | Global Positioning System |
| GCM | Global Climatic Model |
| HEC-HMS | Hydrologic Engineering Center-Hydrologic Modeling System |
| HEC-SSP | Hydrologic Engineering Center-Statistical Software Package |
| HPE | High Precipitation Events |
| HY-8 | Culvert Hydraulic Analysis Program |
| LULC | Land Use Land Cover |
| NMS | Nablus Meteorological Station |
| NRCS | Natural Resources Conservation Service |
| NSE | Nash-Sutcliffe Efficiency |
| PBIAS | Percent Bias |
| RCM | Regional Climate Model |
| SCS | Soil Conservation Services |
| UH | Unit Hydrograph |
| USACE | United States Army Corps of Engineers |
| WWTP | Wastewater Treatment Plant |

# References


Abbas, M., Zhao, L., & Wang, Y. (2022). Perspective Impact on Water Environment and Hydrological. *The Journal of Hydrology*.

Abu Jafal, Y., Hmeidan, M., Bitar, S., & Abu-Salameh, R. (2023). *Nablus Western WWTP Monthly Report.*

Almazroui, M., Islam, M., & Jones, P. (2023). Projected changes in extreme precipitation events in the Eastern Mediterranean region under global warming scenarios. *Climate Dynamics*.

Alpert, P. (2004). The water crisis in the E. Mediterranean – and relation to global warming.

Alpert, P., Ben-Gai, T., Bahard, A., Benjamini, Y., Yekutiele, D., Colacino, M., . . . Manes, A. (2002). The paradoxical increase of Mediterranean extreme daily rainfall in spite of decrease in total values. *Geophysical Research Letters*.

AQUA Consulting Center. (2013). *Rehabilitation of Wadi Al Zeimar - Anabta.* Nablus.

Architects, A. J. (2008). *Regional Wastewater Disposal Tulkarem-Consultancy Services for Review of Feasability Study.*

ARIJ, A. (1996). *Environmental Profile for the West Bank.*

ARIJ, A. R. (2015). *Status of the Environment in the State of Palestine.*

ASCE, A. S. (2013). *The New Handbook of Hydrology.*

Assaf, H., Paola, M., Pinhas, A., & Hadas, S. (2018, May 9). High-Resolution Projection of Climate Change and Extremity Over Israel using COSMO-CLM.

Awati, R. (2015). *GIGO*. Retrieved from TechTarget: https://www.techtarget.com/searchsoftwarequality/definition/garbage-in-garbage-out

B. J., S. B., & W. M. (2009). *Review of Hydrologic Models for Forest MAnagement and Climate Change Applications in British Columbia and Alberta.*

Bahremand, A., & De Smedt, F. (2006). Sensitivity and Uncertainty Analysis of the WetSpa Model Using PEST. *Proceedings of the 2006 IASME/WSEAS Int. Conf. on Water Resources,Hydraulics and Hydrology*, (pp. 26-35). Greece.

Balasubramanian, A. (2017). *Digital Elevation Model DEM in GIS.*

Baths, I. (2023). *A Short History of Sinks*. Retrieved from ICO Baths: https://icobath.com/a-short-history-of-sinks/?doing_wp_cron=1697434507.1578240394592285156250#:~:text=Those%20basins%20were%20just%20basins,%2C%20go%20under%2C%20or%20subside.

Becker, N., Friedler, E., & Haddad, M. (2007). *The Alexander River - Wadi Zeimar Basin ; Palestinian - Israeli Case Study.* Optima.

Bigiarini, M. Z. (2010). *PBIAS HydroGOF.* Retrieved from Search Project: https://search.r-project.org/CRAN/refmans/hydroGOF/html/pbias.html#:~:text=Percent%20bias%20(PBIAS)%20measures%20the,values%20indicating%20accurate%20model%20simulation.

Bigiarini, M. Z. (2010). *PBIAS HydroGOF.* Retrieved from Search Project: https://search.r-project.org/CRAN/refmans/hydroGOF/html/pbias.html#:~:text=Percent%20bias%20(PBIAS)%20measures%20the,values%20indicating%20accurate%20model%20simulation.

Canada, G. o. (n.d.). Retrieved from nrcan.gc.ca: https://www.nrcan.gc.ca/maps-tools-and-publications/satellite-imagery-and-air-photos/tutorial-fundamentals-remote-sensing/educational-resources-applications/land-cover-biomass-mapping/land-cover-land-use/9373

Ceballos, G., Fernandez, J. M., & Ugidos, M. A. (2003). Analysis of rainfall trends and dry. *Journal of Arid Enviroments*.

Christierson, B., Vidal, J., & Wade, S. (2012). Using UKCP09 probabilistic climate information for UK water resource planning. *The Journal of Hydrology*.

Climate Service Center. (2015). *Climate fact sheet Israel-Jordan-Lebanon-Palestine-Syria.*

Corvallis Forestry Research Community. (2006). Retrieved from https://www.fsl.orst.edu/geowater/FX3/help/8_Hydraulic_Reference/Manning_s_Equation.htm

Cunderlik, J., & Simonovic, S. (2004). *Calibration, verification, and sensitivity analysis of the HEC-HMS hydrologic model.* The University of Western Ontario.

Daniel, B. E., Camp, J. V., LeBoeuf, E. J., Penrod, J. R., Dobbins, J. P., & Abkowitz, M. D. (2011). Watershed Modeling and its Applications: A State-of-the-Art Review. *The Open Hydrology Journal*, 25.

Darawosheh, A. (2014). *Spatial quality of municipal wastewater flowing in wadi Al Zomar and infiltrated through wadi bed* .

Department of Environment and Science, Q. (2021). *Hydrology - Catchment and Subcatchment*. Retrieved from Wetland Info: https://wetlandinfo.des.qld.gov.au/wetlands/ecology/processes-systems/water/hydrology/landscape.html

Doan, C., Jiandong, L., Sanders, R., Liong, S.-Y., Dao, A., & Fewtrell, T. (2015). Regional frequency analysis of extreme rainfall events in Jakarta. *Natural Hazards: Journal of the International Society for the Prevention and Mitigation of Natural Hazards*.

Dotan, P., Yeshayahu, M., Odeh, W., Gordon-Kirsch, N., Groisman, L., Al-Khateeb, N., . . . Arnon, S. (2017). Endocrine disrupting compounds in streams in Israel and

the Palestinian West Bank: Implications for transboundary basin management. *Journal of Environmental Management*, 355-364.

Eltahir, E., & Pal, J. (2022). Projected changes in temperature and precipitation extremes over the Middle East and North Africa by the end of the 21st century. *Climate Dynamics*.

Feldman, A., & Hydrologic Engineering Center U.S. (2022). *Hydrologic Modeling System HEC-HMS: Technical Reference Manual.* Retrieved from HEC USACE Military: https://www.hec.usace.army.mil/confluence/hmsdocs/hmsum/4.11

Fonseca, A., & Santos, J. (2019). Predicting hydrologic flows under climate change: The Tâmega Basin as an analog for the Mediterranean. *Science of the Total Environment* .

Freeze, R., & Stephenson, G. (1974). *Mathematical Simulation of Subsurface Flow Contributions to Snowmelt Runoff, Reynolds Creek Watershed, Idaho.*

Gandi, S., & Sarkar, B. (2016). Reconnaissance and Prospecting. In *Essentials of Mineral Exploration and Evaluation.*

Government, C. (n.d.). Retrieved from Government of Canada Website.

Government, P. M. (2023). *GeoMOLG: Geographic Information System for Municipalities [Geodatabase]*. Retrieved from geomolg.ps

Hammed, A., Mohsen, M., & Nazzal, O. (2011). *Rainfall-Runoff Modeling of Wadi Zimar.*

Hayes, A. (2023). *Chi-Square (χ2) Statistic: What It Is, Examples, How and When to Use the Test.* Retrieved from Investopedia: https://www.investopedia.com/terms/c/chi-square-statistic.asp

Hochman, A., Bucchingnani, E., Gershtein, G., Krichak, S., Alpert, P., Levi, Y., . . . Mercogliano, P. (2017). Evaluation of seasonal COSMO-CLM climate simulations over the Eastern Mediterranean for the period 1979-2011. *International Journal of Climatology*.

Hochman, A., Mercogliano, P., Alpert, P., Saaroni, H., & Bucchignani, E. (2018). High-Resoution Projection of Climate Change and Extremity Over Israel Using COSMO-CLM. *International Journal of Climatology*.

Houghton, J. T., Meira Filho, L. G., Callander, B. A., Harris, N., Kattenberg, A., & Maskell, K. (1995). *Climate Change : The Science of Climate Change.* Cambridge University Press.

*Hydraulic Reference - Manning Equation*. (2004). Retrieved from Corvallis Foresty Research Community: https://www.fsl.orst.edu/geowater/FX3/help/8_Hydraulic_Reference/Manning_s_Equation.htm

ICRC, I. C. (2021). *Israel and the Occupied Territories - Climate Fact Sheet.*

Ikenberry, C. (n.d.). *Nash-Sutcliffe Model Efficiency Coefficient*. Retrieved from GoldSim Help Center: https://support.goldsim.com/hc/en-us/articles/360012774094-Nash-Sutcliffe-Model-Efficiency-Coefficient#:~:text=The%20Nash%2DSutcliffe%20model%20efficiency,loadings%2C%20temperature%2C%20concentrations%20etc.

IMS, I. M. (2023). *Meteorological Database.* Retrieved from https://ims.gov.il/en/data_gov

Klemes, V. (1986). Operational Testing of Hydrological Simulation Models. *Hydrol. Sci. J.*, 13-24.

Ladson, A. (2008). *Hydrology An Australian Introduction.* Australia: Oxford University Press.

Leeper, G., & Uren, N. (1993). *Soil Science, An Introduction. 5th edition.*

Lionello, A., Gacic, M., Planton, S., Trigo, R., & Ulbrich, U. (2014). *The climate of the Mediterranean region: Research progress and climate change impacts.* Regoinal Environmental Change.

Lohani, D. A. (2016). *Rainfall - Runoff Analysis and Modeling.*

Lohani, D. A. (2016). *Rainfall - Runoff Analysis and Modeling.*

Luijten, J., Jones, J., & Knapp, E. (2002). *Spatial Water Budget Model and GIS Hydrological Tools, ICASA.* International Consoritum for Agricultutral Systems Applications.

Maidment, D. (2019). *Handbook of Hydrology.* McGraw-Hill Education.

Maidment, D. R. (2007). *The Handbook of Hydrology.*

Martinez-Carreras, N., Hissler, C., Gourdol, L., Klaus, J., Jullieret, J., Francois ffly, J., . . . Pfister, L. (2016). On the Trial of Double Peak Hydrographs. *EGU General Assambly.* Vienna.

Mihalik, N., Levine, S., & Amatya, M. (2008). Rainfall-Runoff Modeling of Chapel Branch Creek Watershed using GIS-based Rational and SCS-CN Methods.

Moss, R., Edmonds, J., Hibbard, K., Manning, M., Rose, S., Van Vuuren, D., . . . Kram, T. (2010). *The next generation of scenarios for climate change research and assessment* .

National Oceanic and Atmospheric Adminstration. (2023). *The Hydrologic Cycle*. Retrieved from NOAA: https://www.noaa.gov/jetstream/atmosphere/hydro

Niazkar, M., & Zakwan, M. (2022). Parameter estimation of a new four-parameter Muskingum flood routing model. In *Computers in Earth and Environmental Sciences.*

Olofintoye, O., Sule, B., & Salami, A. (2009). Best-fit Probability Distribution model for peak daily rainfall of selected Cities in Nigeria. *New York Science Journal*.

Palestinian Central Bereau of Statistics PCBS. (2023). *Population Statistics*. Retrieved from https://www.pcbs.gov.ps/statisticsIndicatorsTables.aspx?lang=en&table_id=697

Palestinian Meteorological Department. (2024). *Climate Information*. Retrieved from https://www.pmd.ps/en

Palestinian Water Authority (PWA). (2024). *Palestinian Water Authority-Projects*. Retrieved from Palestinian Water Authority: https://www.pwa.ps/projects.aspx

Parry, M., Canziani, O., Palutikof, J., Linden, P. V., & Hanson, C. (2007). *Climate Change 2007: Impacts, Adaptation and Vulnerability.* IPCC.

Pe'er, G., & Safriel, U. N. (2000). *Climate Change: Impact, Vulnerability and Adaptation.* Israel National Report under the United Nations Framework Convention on Climate Change (UNFCCC).

Rice, E. (1886). Rainfall in Palestine. *Journal of the Society of Biblical Literature and Exegesis*, 69-72.

Rofe and Raffety Consulting Engineers. (1965). *West Bank Hydrology: Nablus District water resources survey, geological and hydrolodical report.*

Sajikumar, N., & Remya, R. (2015). Impact ofLand Cover andLand Use Change on Runoff Characteristics. *Journal of Environmental Management*, 460–468.

SATPALDA. (2018, 07 07). *Significance of Land Use / Land Cover LULC Maps*. Retrieved from SATPALDA: https://www.satpalda.com/blogs/significance-of-land-use-land-cover-lulc-maps

Sen, Z. (2008). *Wadi Hydrology.* Istanbul: CRC Press - Taylor and Francis Group.

Shadeed, S. (2013). *Climate Changes and Trends in Rainfall and Temperature of Nablus.*

Shadeed, S. (2019). Hydrologic Analysis. In D. S. Shadeed.

Sharif, H., Mahmood, T., & Nasiri, M. (2021). Application of HEC-HMS for flood forecasting and management: A case study of Johor River Basin, Malaysia. *Environmental Earth Sciences*.

Siegfried, T., & Marti, B. (2021). *Applied Hydrological Modeling.* Zurich.

Singh, V. P. (1995). *Computer Models of Watershed Hydrology.*

Singh, V. P., & Woolhiser, D. A. (2002). Mathematical Modelilng of Watershed Hydrology. *American Society of Civil Engineers*, 23.

Smemoe, C. (2022). *HY-8 User Manual (Version 7.5).* FHWA.

Tayfur, G. (2023). Real-time flood hydrograph predictions using rating curve and soft computing methods (GA, ANN). In *Handbook of Hydroinformatics.*

U.S. Army Corps of Engineers. (2022). *HEC-HMS Tutorials and Guidelines*. Retrieved from https://www.hec.usace.army.mil/confluence/hmsdocs/hmsguides/applying-reach-routing-methods-within-hec-hms/applying-the-muskingum-routing-method

UNDP. (2010). *Climate Change adaptation strategy and programme of action for teh Palestinian Authority.*

United Nations Development Programme. (2020). *Climate Change Profile - Palestinian Territories.* Retrieved from https://www.adaptation-undp.org/explore/mashreq/palestine/314-climate-change-profile-palestinian-territories

United States Department of Agriculture. (2021). National Engineering Handbook.

University, U. S. (n.d.). Retrieved from EPA: chrome-extension://efaidnbmnnnibpcajpcglclefindmkaj/https://www.epa.gov/sites/default/files/2015-07/documents/lecture-3-watershed-delineation.pdf

Verma, A. K., Jha, M. K., & Mahana, R. K. (2009, December 3). Evaluation of HEC-HMS and WEPP for simulating watershed. p. 131.

*Weather Underground*. (n.d.). Retrieved from www.weatherunderground.com

Weshah, R. A. (2010). *RAINFALL-RUNOFF ANALYSIS AND MODELING IN WADI SYSTEMS.*

Whaeater, H., & Al-Weshah, R. (2002). *Hydrology of Wadi System - IHP Regional Network on Wadi Hydrology in the Arab Region.* UNESCO.

WSDOT. (2023). *Hydraulics Manual - Culvert Design.* Washington State Department of Transportation.

Zayed, M., & Saadeh, W. (2011). *Hydrologic Study and Flood Mapping of Wadi Zeimar-Anabta.*

Zhang, X., Alexander, L., Hegerel, C., Jones, P., Tank, A., & Peterson, T. (2011). *Indices for monitoring changes in extremes based on daily temperature and precipitation data.*

# Appendices

## Appendix A

## Figures

**Figure A.1**
*Al Zeimar Catchment Location and DEM*

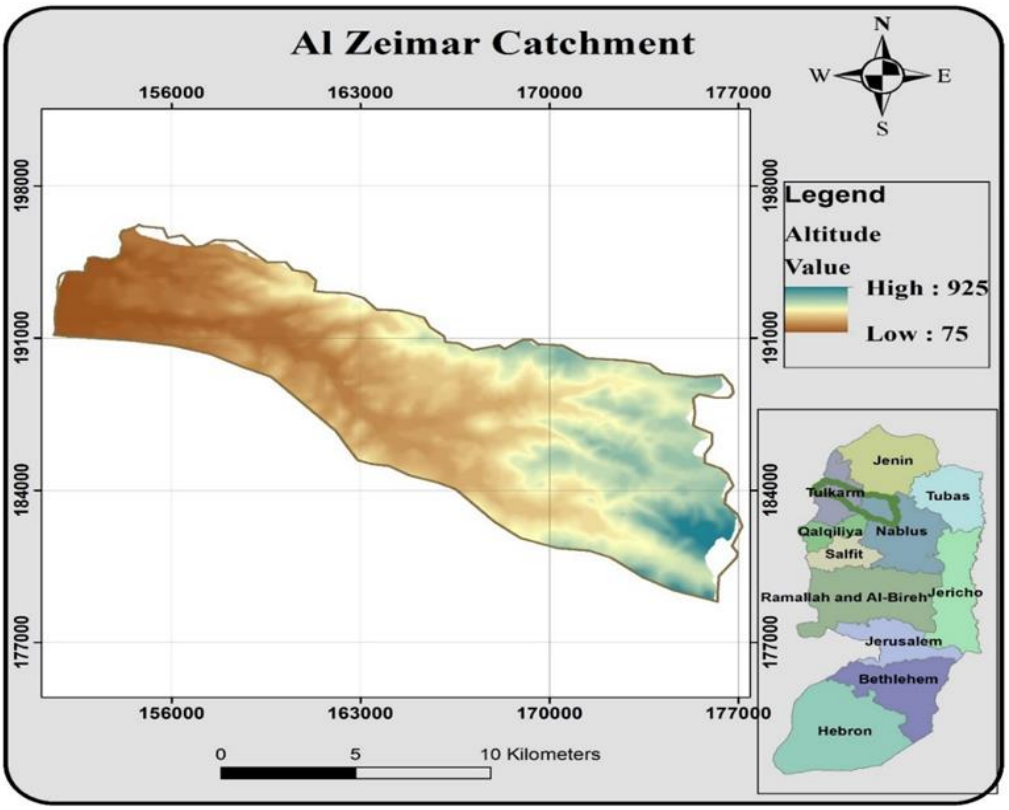

**Figure A.2**

*Al Zeimar Communities*

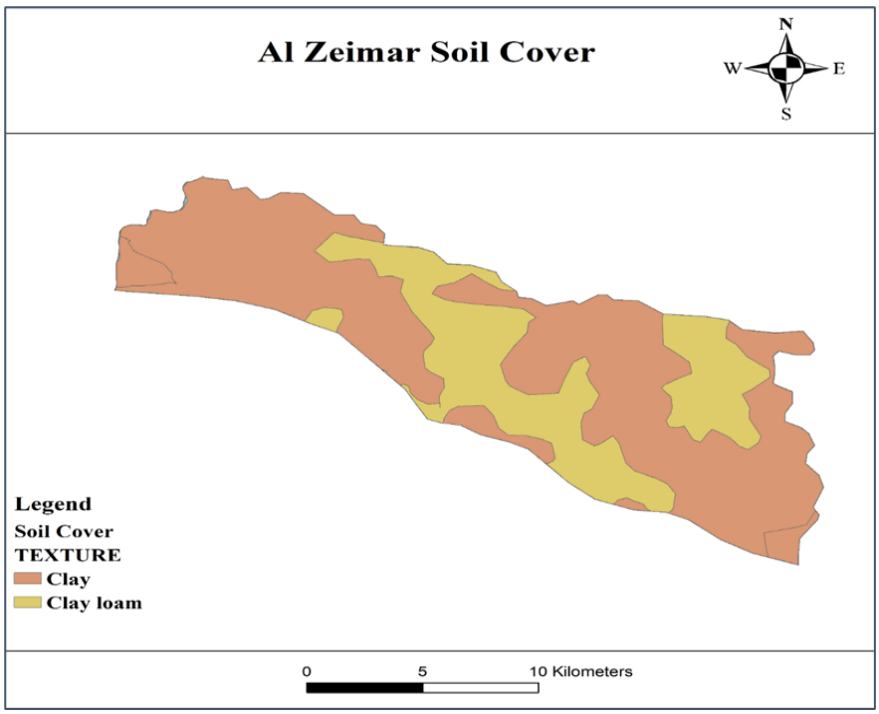


**Figure A.3**

*Al Zeimar Catchment Soil Cover*

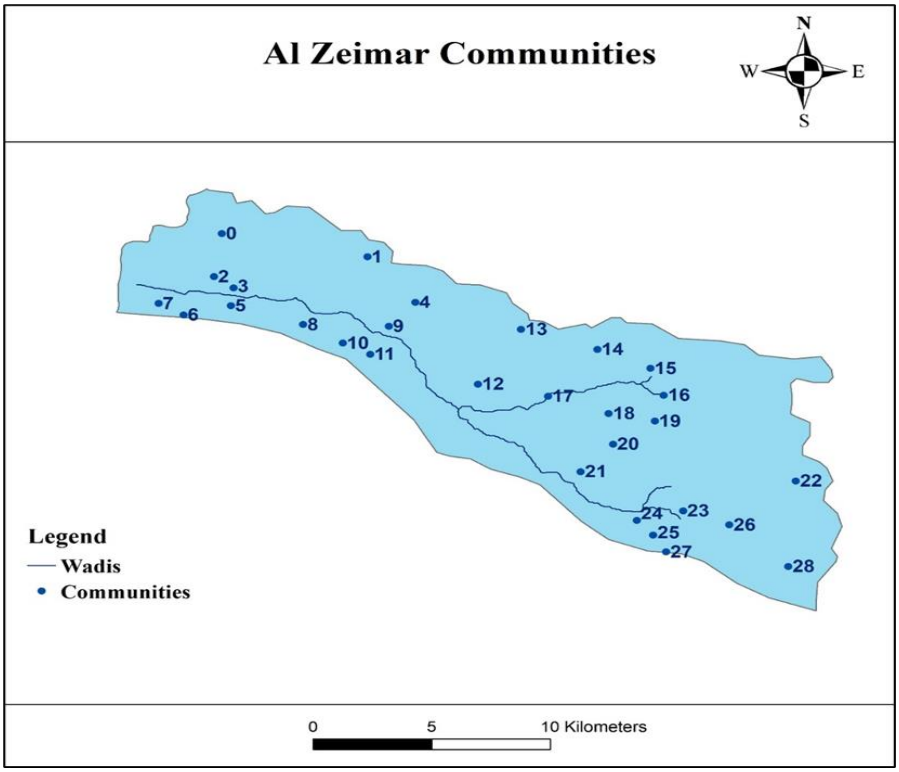

**Figure A.4**

*Al Zeimar Land Use*

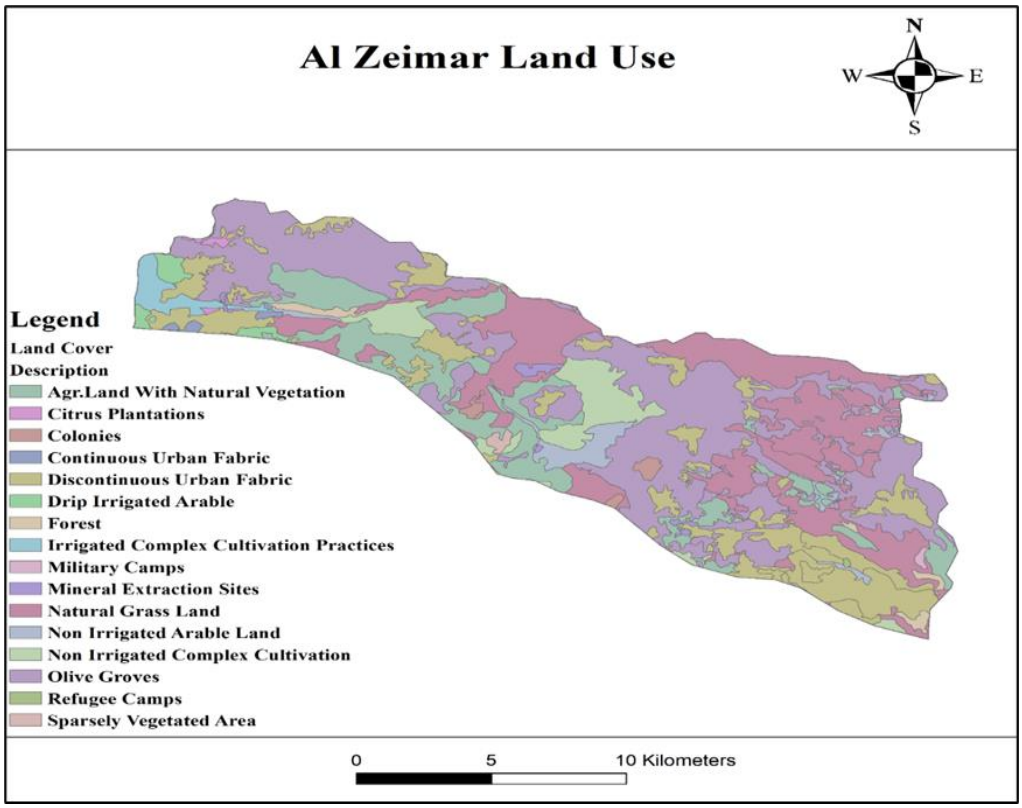


**Figure A.5**

*AL Zeimar Catchment Wadis*

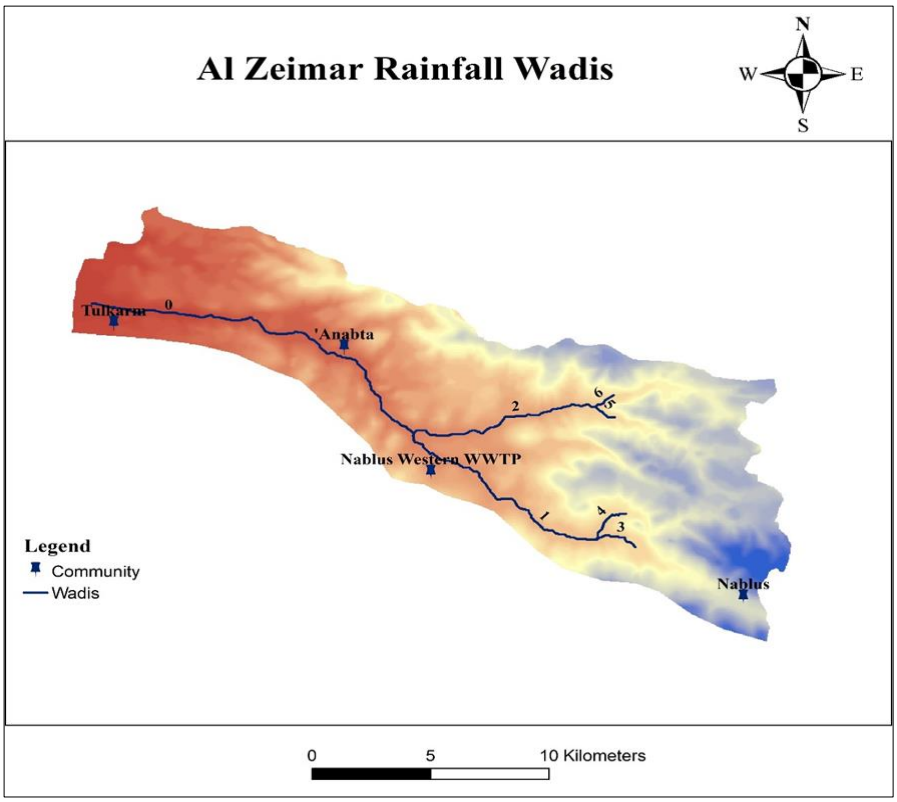

**Figure A.6**

*Average Annual Temperatures of Summer and Winter for the Nablus Station*

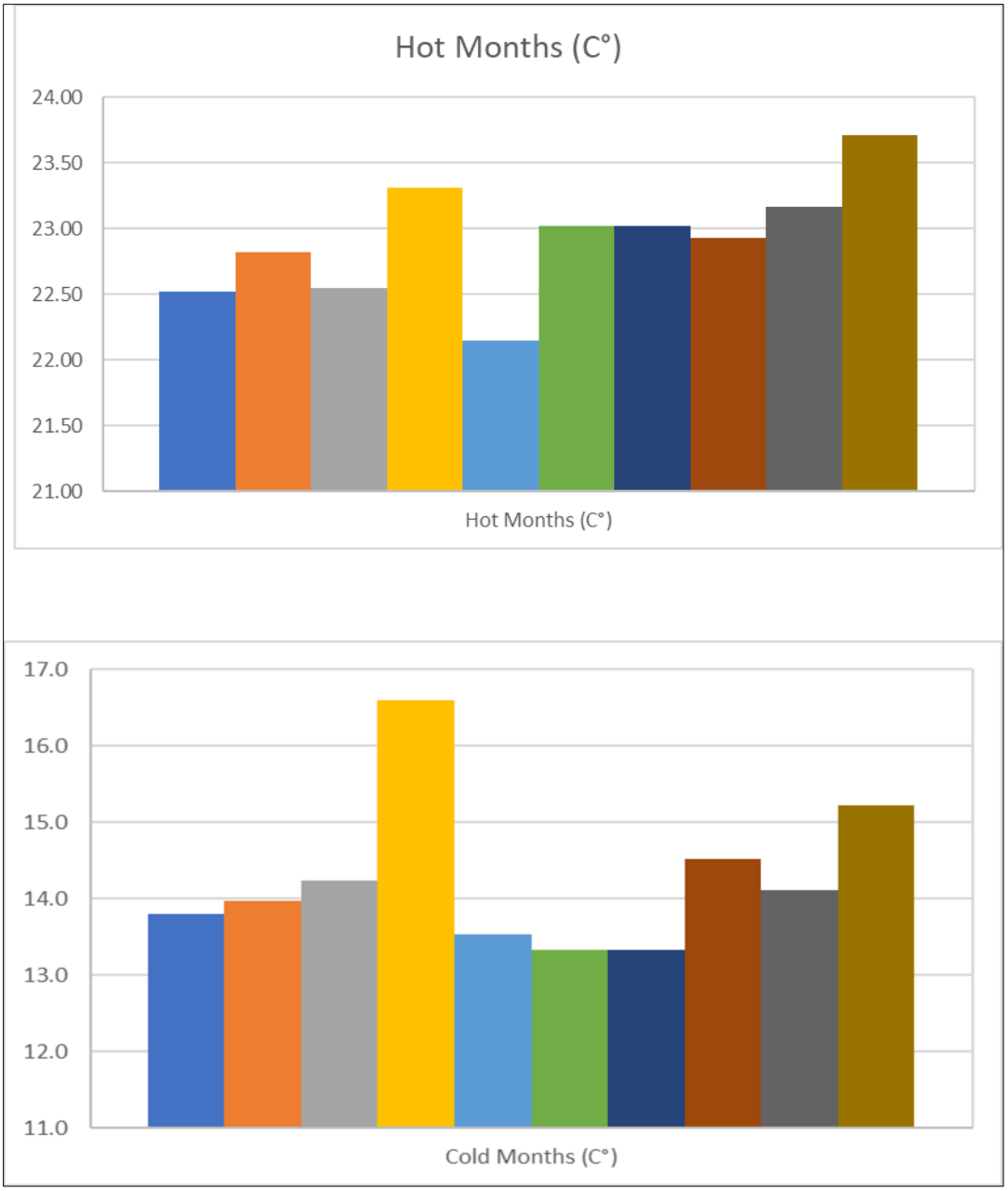

**Figure A.7**

*Average Annual Rainfall of Nablus*

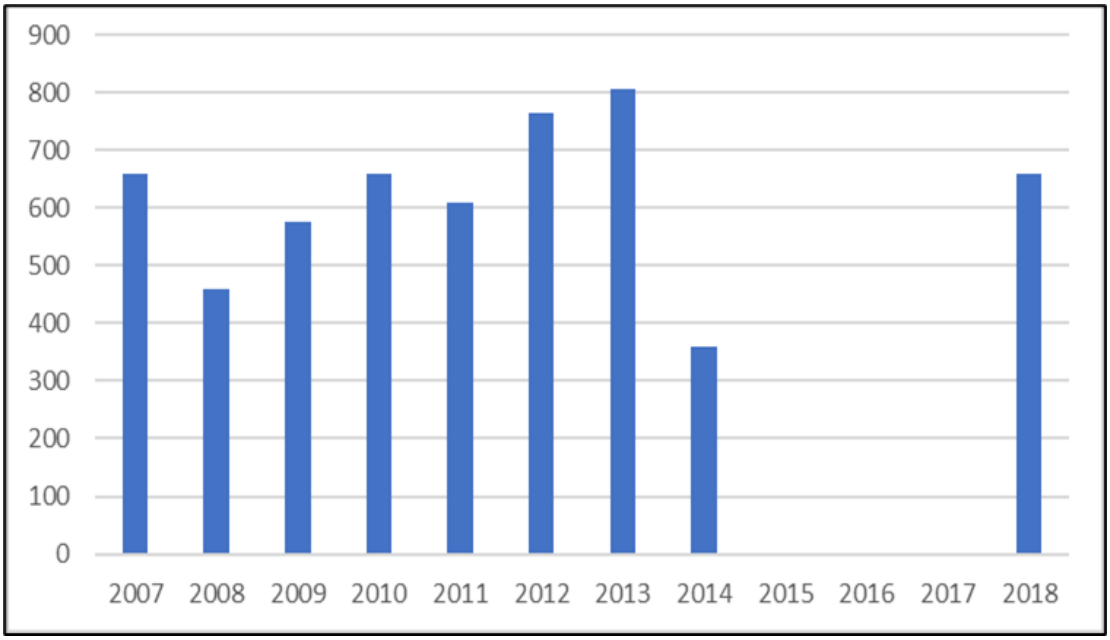


**Figure A.8**

*Number of Rainy Days of Nablus Station*

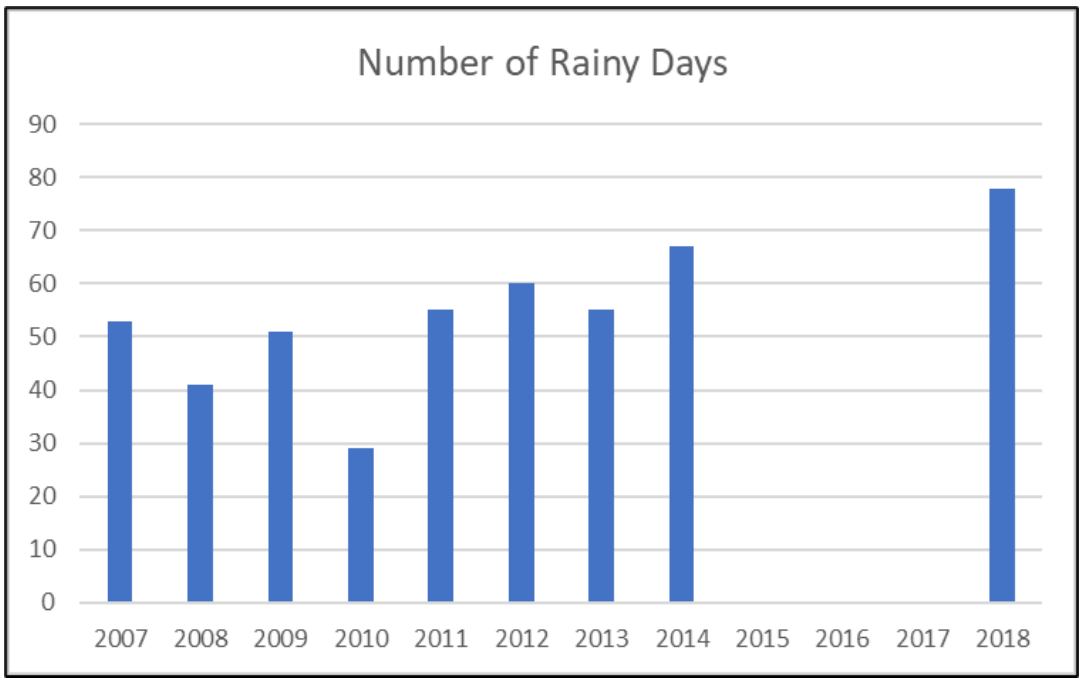

**Figure A.9**

*Average Annual Precipitation of Tulkarm*

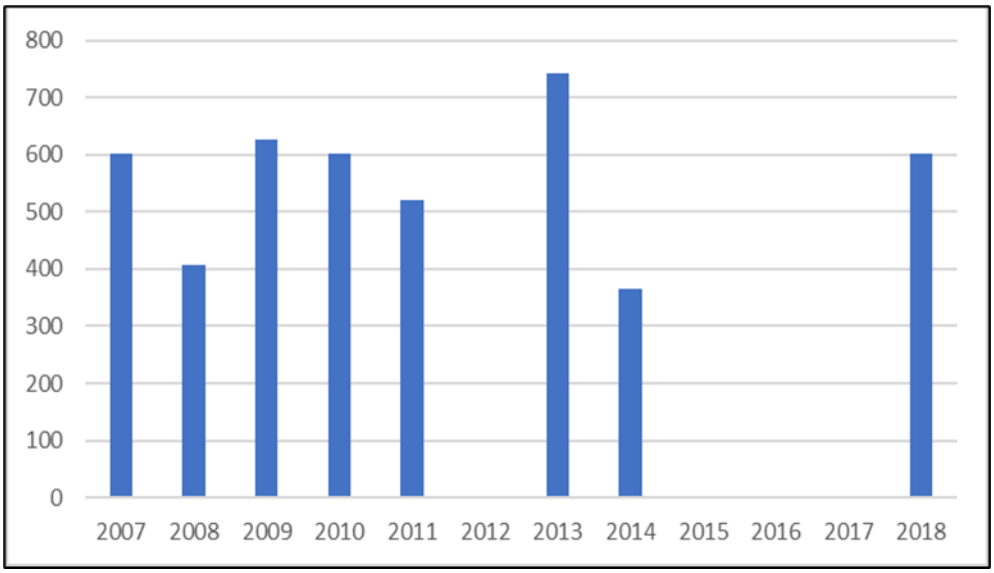


**Figure A.10**

*Al Zeimar Rainfall Contours*

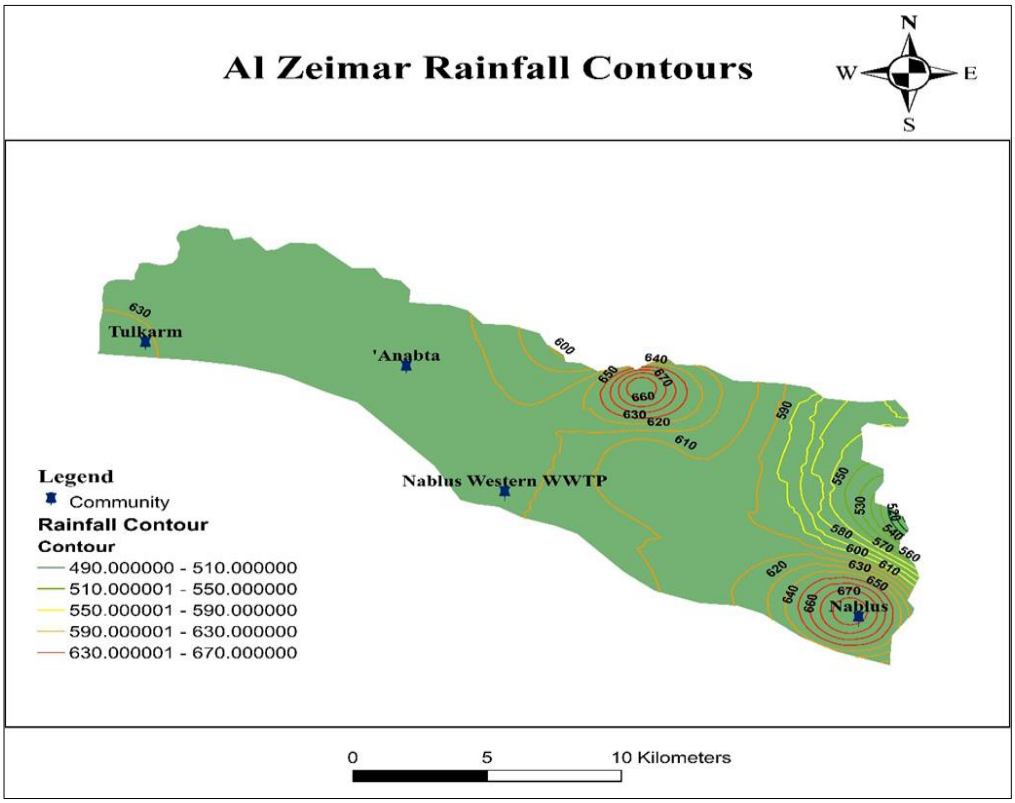

**Figure A.11**
*Methodology Flow Chart*

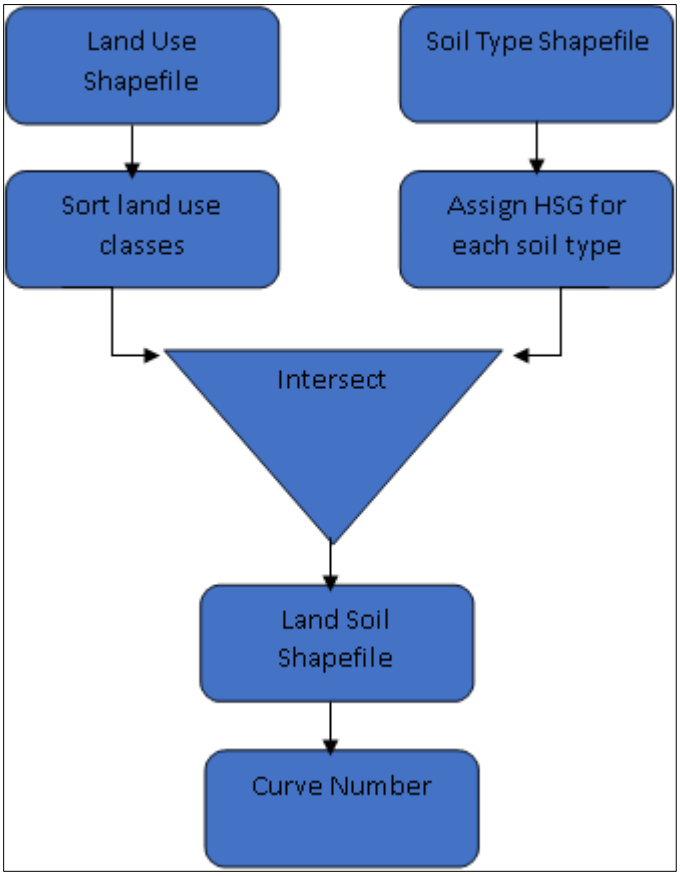

**Figure A.12**

*Al Zeimar Catchment Sink-Partial Flume*

**Figure A.13**

*Hyetograph of Storm 1*

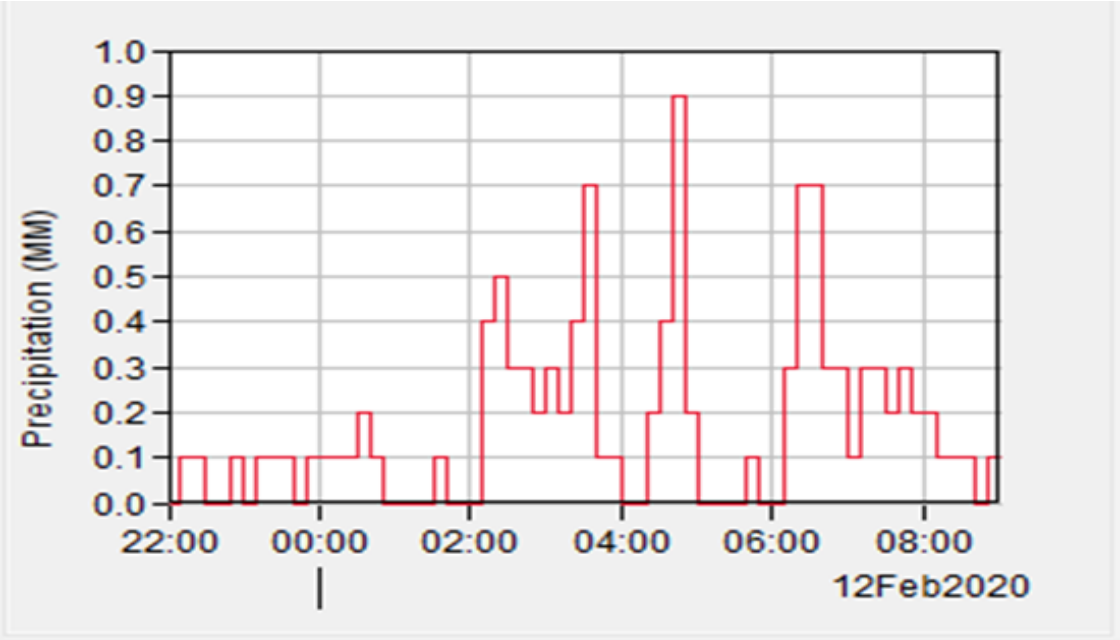

**Figure A.14**

*Storm 1 Hydrograph*

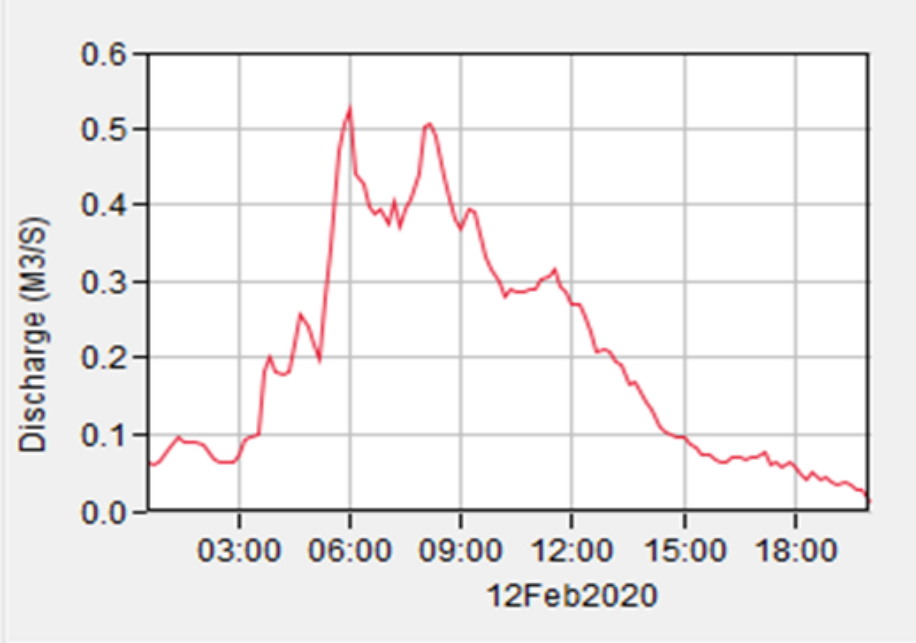


**Figure A.15**

*Built Up Section of Al-Zeimar Stream in Anabta*

**Figure A.16**

*Alexa Storm Hyetograph*

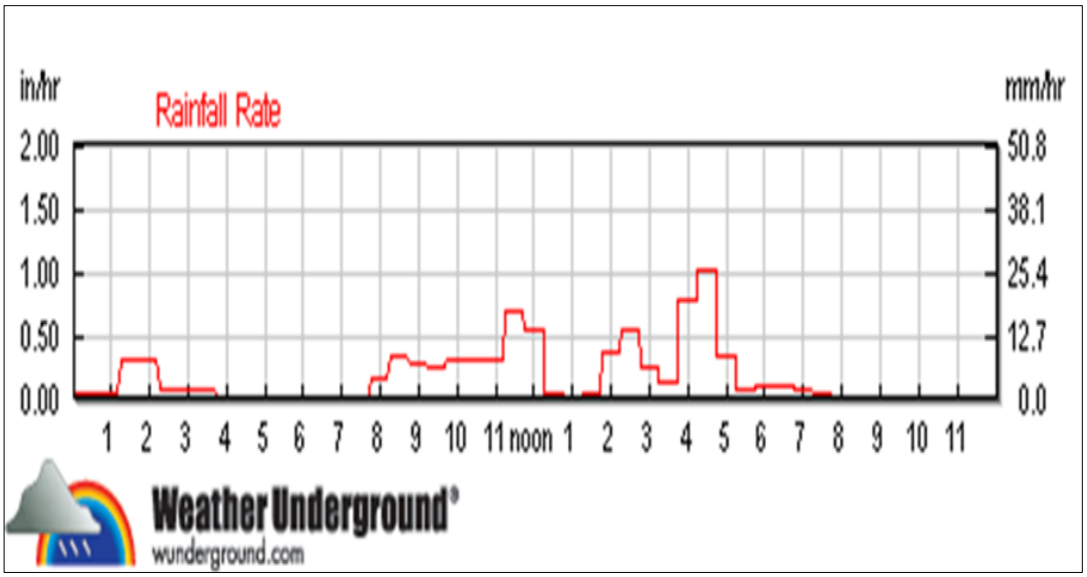


**Figure A.17**

*Aerial View of Al Zeimar Stream*

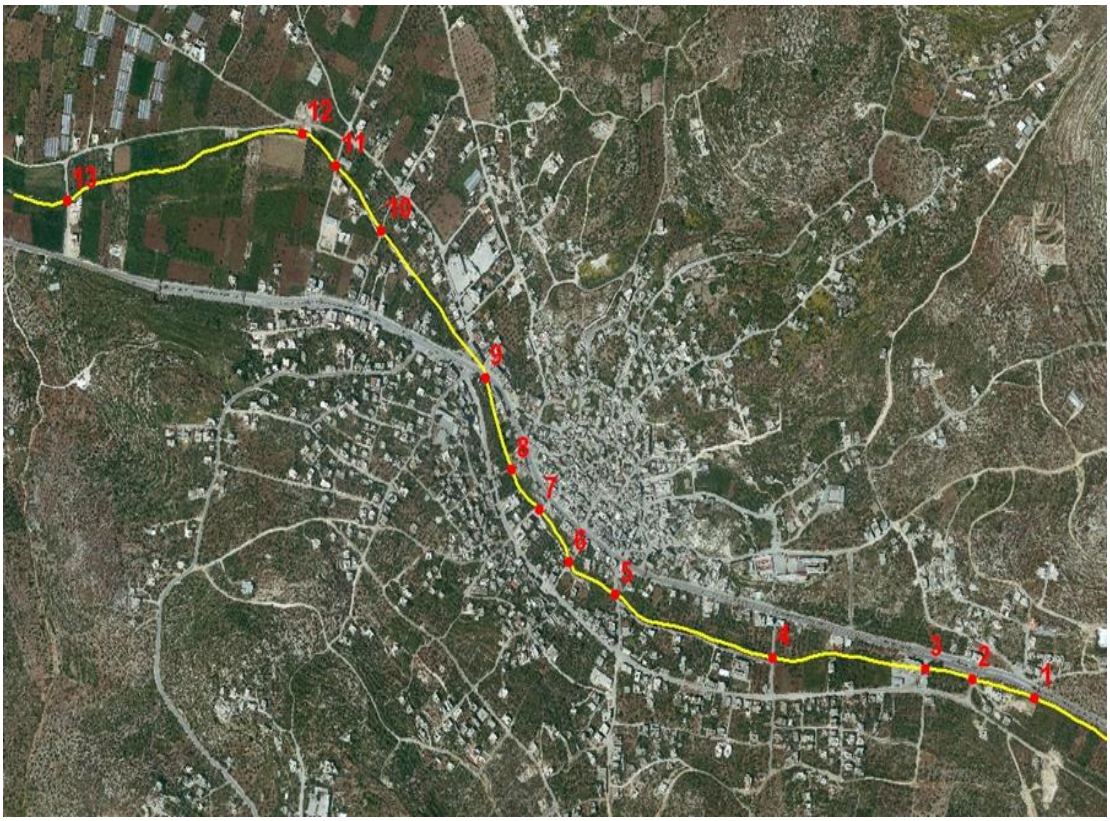

**Figure A.18**

*Culvert in Anabta*

# Appendix B

# Tables

**Table B.1**

*Communities within Al Zeimar*

| ID | Community | Population |
|---|---|---|
| 0 | Al Jarushiya | 1305 |
| 1 | Bal'a | 8626 |
| 2 | Iktaba | 3305 |
| 3 | Nur Shams Camp | 7083 |
| 4 | Kafr Rumman | - |
| 5 | Camp Tulkarm | 10951 |
| 6 | Dhinnaba | - |
| 7 | Tulkarm | 71161 (Including 4, 6, 8) |
| 8 | 'Izba Abu Khameis | - |
| 9 | Anabta | 8907 |
| 10 | 'Izbat al Khilal | 154 |
| 11 | Kafr al Labad | 5235 |
| 12 | Ramin | 2203 |
| 13 | Bizzariya | 3105 |
| 14 | Burqa | 4615 |
| 15 | Beit Imrin | 3693 |
| 16 | Nisf Jubeil | 523 |
| 17 | Al Mas'udiya | - |
| 18 | Sabastiya | 3562 (Including ID.17) |
| 19 | Ijnisinya | 650 |
| 20 | An Naqura | 1985 |
| 21 | Deir Sharaf | 3278 |

| | | |
|---|---|---|
| 22 | 'Asira ash Shamaliya | 9795 |
| 23 | Zawata | 2820 |
| 24 | Beit Iba | 4533 |
| 25 | Beit Wazan | 1458 |
| 26 | 'Ein Beit el Ma Camp | 3988 |
| 27 | Al Juneid | - |
| 28 | Nablus | 174387 (Including 27) |

**Table B.2**

*Soil Types within Al Zeimar*

| Soil Type | Soil Texture | Area ($Km^2$) | Description |
|---|---|---|---|
| Brown Rendzinas and Pale Rendzinas | Clay Loam | 54.63 | Covers the area from the effluent point in Nablus to Anabta |
| Terra Rossa, Brown Rendzinas and Pale Rendzinas | Clay | 113.2 | Covers the area from Anabta to Tulkarem |
| Grumusols | Clay | 4.64 | Small Area closed to the green line |

**Table B.3**

*Land Use Within Al Zeimar*

| Land Use | Area $km^2$ |
|---|---|
| Agricultural Land with Natural Vegetation | 17.65 |
| Citrus Plantations | 0.09 |
| Colonies | 1.06 |
| Continuous Urban Fabric | 0.35 |
| Discontinuous Urban Fabric | 22.48 |
| Drip Irrigated Arable Land | 0.35 |

| | |
|---|---|
| Forest | 0.91 |
| Irrigated Complex Cultivation Practices | 1.09 |
| Military Camps | 0.19 |
| Mineral Extraction Sites | 0.87 |
| Natural Grass Land | 36.76 |
| Non-Irrigated Arable Land | 4.02 |
| Non-Irrigated Complex Cultivation | 8.93 |
| Olive Groves | 40.77 |
| Refugee Camps | 0.07 |
| Sparsely Vegetated Area | 0.43 |

**Table B.4**

*Wadis within Al Zeimar*

| Wadi ID | Name | الاسم |
|---|---|---|
| 0 | Zeimar and Burj | زيمار والبرج |
| 1 | Shei'r and Qusin | الشعير وقوصين |
| 2 | Shami | الشامي |
| 3 | Beit Eba | بيت ايبا |
| 4 | Mousa | موسى |
| 5 | Qate'lo | قاطعلو |
| 6 | Hajja | الحجة |

**Table B.5**

*CN Tables*

(a) Cultivated Agricultural Lands [1/]

| Cover Description | | Hydrologic Condition [3/] | Runoff Curve Numbers for Hydrologic Soil Group | | | |
|---|---|---|---|---|---|---|
| Cover Ttype | Treatment [2/] | | A | B | C | D |
| Fallow | Bare soil | ----- | 77 | 86 | 91 | 94 |
| | Crop residue cover (CR) | Poor | 76 | 85 | 90 | 93 |
| | | Good | 74 | 83 | 88 | 90 |
| Row crops | Straight row | Poor | 72 | 81 | 88 | 91 |
| | | Good | 67 | 78 | 85 | 89 |
| | Straight row + CR | Poor | 71 | 80 | 87 | 90 |
| | | Good | 64 | 75 | 82 | 85 |
| | Contoured (C) | Poor | 70 | 79 | 84 | 88 |
| | | Good | 65 | 75 | 82 | 86 |
| | Contoured + CR | Poor | 69 | 78 | 83 | 87 |
| | | Good | 64 | 74 | 81 | 85 |
| | Contoured & terraced (C&T) | Poor | 66 | 74 | 80 | 82 |
| | | Good | 62 | 71 | 78 | 81 |
| | C&T + CR | Poor | 65 | 73 | 79 | 81 |
| | | Good | 61 | 70 | 77 | 80 |
| Small grain | Straight row | Poor | 65 | 76 | 84 | 88 |
| | | Good | 63 | 75 | 83 | 87 |
| | Straight row + CR | Poor | 64 | 75 | 83 | 86 |
| | | Good | 60 | 72 | 80 | 84 |
| | Contoured (C) | Poor | 63 | 74 | 82 | 85 |
| | | Good | 61 | 73 | 81 | 84 |
| | Contoured + CR | Poor | 62 | 73 | 81 | 84 |
| | | Good | 60 | 72 | 80 | 83 |
| | Contoured & terraced (C&T) | Poor | 61 | 72 | 79 | 82 |
| | | Good | 59 | 70 | 78 | 81 |
| | C&T + CR | Poor | 60 | 71 | 78 | 81 |
| | | Good | 58 | 69 | 77 | 80 |
| Close-seeded or broadcast legumes or rotation meadow | Straight row | Poor | 66 | 77 | 85 | 89 |
| | | Good | 58 | 72 | 81 | 85 |
| | Contoured (C) | Poor | 64 | 75 | 83 | 85 |
| | | Good | 55 | 69 | 78 | 83 |
| | Contoured & terraced (C&T) | Poor | 63 | 73 | 80 | 83 |
| | | Good | 51 | 67 | 76 | 80 |

(b) Other Agricultural Lands [1/]

| Cover Description | Hydrologic Condition | Runoff Curve Numbers for Hydrologic Soil Group | | | |
|---|---|---|---|---|---|
| Cover Type | | A | B | C | D |
| Pasture, grassland, or range—continuous forage for grazing [2/] | Poor | 68 | 79 | 86 | 89 |
| | Fair | 49 | 69 | 79 | 84 |
| | Good | 39 | 61 | 74 | 80 |
| Meadow—continuous grass, protected from grazing and generally mowed for hay | ----- | 30 | 58 | 71 | 78 |
| Brush—brush-forbs-grass mixture with brush the major element [3/] | Poor | 48 | 67 | 77 | 83 |
| | Fair | 35 | 56 | 70 | 77 |
| | Good | 30 [4/] | 48 | 65 | 73 |
| Woods-grass combination (orchard or tree farm) [5/] | Poor | 57 | 73 | 82 | 86 |
| | Fair | 43 | 65 | 76 | 82 |
| | Good | 32 | 58 | 72 | 79 |
| Woods [6/] | Poor | 45 | 66 | 77 | 83 |
| | Fair | 36 | 60 | 73 | 79 |
| | Good | 30 [4/] | 55 | 70 | 77 |
| Farmsteads—buildings, lanes, driveways, and surrounding lots | ----- | 59 | 74 | 82 | 86 |

(c) Arid and Semiarid Rangelands [1/]

| Cover Description | Hydrologic Condition [2/] | Runoff Curve Numbers for Hydrologic Soil Group | | | |
|---|---|---|---|---|---|
| Cover Type | | A [3/] | B | C | D |
| Herbaceous – mixture of grass, weeds, and low-growing brush, with brush the minor element | Poor | | 80 | 87 | 93 |
| | Fair | | 71 | 81 | 89 |
| | Good | | 62 | 74 | 85 |
| Oak-aspen – mountain brush mixture of oak brush, aspen, mountain mahogany, bitter brush, maple, and other brush | Poor | | 66 | 74 | 79 |
| | Fair | | 48 | 57 | 63 |
| | Good | | 30 | 41 | 48 |
| Pinyon-juniper – pinyon, juniper, or both; grass understory | Poor | | 75 | 85 | 89 |
| | Fair | | 58 | 73 | 80 |
| | Good | | 41 | 61 | 71 |
| Sagebrush with grass understory | Poor | | 67 | 80 | 85 |
| | Fair | | 51 | 63 | 70 |
| | Good | | 35 | 47 | 55 |
| Desert shrub – major plants, include saltbush, greasewood, creosotebush, blackbrush, bursage, palo verde, mesquite, and cactus | Poor | 63 | 77 | 85 | 88 |
| | Fair | 55 | 72 | 81 | 86 |
| | Good | 49 | 68 | 79 | 84 |

(d) Urban Areas [1/]

| Cover Description | Average Percent Impervious Area [2/] | Runoff Curve Numbers for Hydrologic Soil Group | | | |
|---|---|---|---|---|---|
| Cover Type and Hydrologic Condition | | A | B | C | D |
| Fully developed urban areas (vegetation established): | | | | | |
| Open space (lawns, parks, golf courses, cemeteries, etc.): [3/] | | | | | |
| Poor condition (grass cover < 50%) | | 68 | 79 | 86 | 89 |
| Fair condition (grass cover 50% to 75%) | | 49 | 69 | 79 | 84 |
| Good condition (grass cover > 75%) | | 39 | 61 | 74 | 80 |
| Impervious areas: | | | | | |
| Paved parking lots, roofs, driveways, etc. (excluding right-of-way) | | 98 | 98 | 98 | 98 |
| Streets and roads: | | | | | |
| Paved; curbs and storm sewers | | 98 | 98 | 98 | 98 |
| Paved; open ditches (including right-of-way) | | 83 | 89 | 92 | 93 |
| Gravel (including right-of-way) | | 76 | 85 | 89 | 91 |
| Dirt (including right-of-way) | | 72 | 82 | 87 | 89 |
| Western desert urban areas: | | | | | |
| Natural desert landscaping (pervious areas only) [4/] | | 63 | 77 | 85 | 88 |
| Artificial desert landscaping (impervious weed barrier, desert shrub with 1- to 2- inch sand or gravel mulch and basin borders) | | 96 | 96 | 96 | 96 |
| Urban district: | | | | | |
| Commercial and business | 85 | 89 | 92 | 94 | 95 |
| Industrial | 72 | 81 | 88 | 91 | 93 |
| Residential districts by average lot size: | | | | | |
| 1/8 acre or less (town houses) | 65 | 77 | 85 | 90 | 92 |
| 1/4 acre | 38 | 61 | 75 | 83 | 87 |
| 1/3 acre | 30 | 57 | 72 | 81 | 86 |
| 1/2 acre | 25 | 54 | 70 | 80 | 85 |
| 1 acre | 20 | 51 | 68 | 79 | 84 |
| 2 acres | 12 | 46 | 65 | 77 | 82 |
| Developing urban areas: | | | | | |
| Newly graded areas (pervious areas only, no vegetation) [5/] | | 77 | 86 | 91 | 94 |

**Table B.6**

*Infiltration Rate for each Soil Group*

| Hydrologic Soil Group | Description | Infiltration Rate |
|---|---|---|
| A | Aggregated silts | High |
| B | Sandy loam | Moderate |
| C | Clay Loams | Slow |
| D | Clay | Very Slow |

**Table B.7**

*AMC*

| AMC | Five Day Precipitation | |
|---|---|---|
| | Dormant Season | Growing Season |
| I | < 12.7 mm | < 35.6 mm |
| II | 12.7 – 28 mm | 35.6 – 53.4 mm |
| III | > 28 mm | > 53.4 mm |

**Table B.8**

*Mannings n*

| Surface Material | Manning's Roughness Coefficient - *n* - |
|---|---|
| Asbestos cement | 0.011 |
| Asphalt | 0.016 |
| Brass | 0.011 |
| Brick and cement mortar sewers | 0.015 |
| Canvas | 0.012 |
| Cast or Ductile iron, new | 0.012 |
| Clay tile | 0.014 |
| Concrete - steel forms | 0.011 |
| Concrete (Cement) - finished | 0.012 |
| Concrete - wooden forms | 0.015 |
| Concrete - centrifugally spun | 0.013 |
| Copper | 0.011 |
| Corrugated metal | 0.022 |
| Earth, smooth | 0.018 |
| Earth channel - clean | 0.022 |
| Earth channel - gravelly | 0.025 |
| Earth channel - weedy | 0.030 |
| Earth channel - stony, cobbles | 0.035 |
| Floodplains - pasture, farmland | 0.035 |
| Floodplains - light brush | 0.050 |
| Floodplains - heavy brush | 0.075 |
| Floodplains - trees | 0.15 |
| Galvanized iron | 0.016 |

| | |
|---|---|
| Glass | 0.010 |
| Gravel, firm | 0.023 |
| Lead | 0.011 |
| Masonry | 0.025 |
| Metal - corrugated | 0.022 |
| Natural streams - clean and straight | 0.030 |
| Natural streams - major rivers | 0.035 |
| Natural streams - sluggish with deep pools | 0.040 |
| Natural channels, very poor condition | 0.060 |
| Plastic | 0.009 |
| Polyethylene PE - Corrugated with smooth inner walls | 0.009 - 0.015 |
| Polyethylene PE - Corrugated with corrugated inner walls | 0.018 - 0.025 |
| Polyvinyl Chloride PVC - with smooth inner walls | 0.009 - 0.011 |
| Rubble Masonry | 0.017 - 0.022 |
| Steel - Coal-tar enamel | 0.010 |
| Steel - smooth | 0.012 |
| Steel - New unlined | 0.011 |
| Steel - Riveted | 0.019 |
| Vitrified clay sewer pipe | 0.013 - 0.015 |
| Wood - planed | 0.012 |
| Wood - unplanned | 0.013 |
| Wood stave pipe, small diameter | 0.011 - 0.012 |
| Wood stave pipe, large diameter | 0.012 - 0.013 |

**Table B.9**

*Maximum Daily Rainfall for Nablus Station (1997-2022)*

| Years | Rainfall (mm) Max. Daily |
|---|---|
| 1997 | 74.8 |
| 1998 | 76.2 |
| 1999 | 53.3 |
| 2000 | 80.2 |
| 2001 | 70 |
| 2002 | 230.7 |
| 2003 | 416.4 |

| | |
|---|---|
| 2004 | 67.9 |
| 2005 | 95 |
| 2006 | 105 |
| 2007 | 43.3 |
| 2008 | 76.8 |
| 2009 | 67.9 |
| 2010 | 83.4 |
| 2011 | 46 |
| 2012 | 74.8 |
| 2013 | 123 |
| 2014 | 55 |
| 2015 | 82.5 |
| 2016 | 73.8 |
| 2017 | 45 |
| 2018 | 89.5 |
| 2019 | 116.9 |
| 2020 | 52.8 |
| 2021 | 73.9 |
| 2022 | 50 |

جـامعـــة النجاح الوطنية

كليـــة الدراســـات العليـــا

# نمذجة جريان المياه في مستجمع وادي الزيمار مع الأخذ في الاعتبار التغير المناخي

إعداد

شهد عبد الحكيم يوسف بيشاوي

إشراف

د. محمد نهاد المصري

قدمت هذه الرسالة استكمالا لمتطلبات الحصول على درجة الماجستير في هندسة المياه والبيئة، من كلية الدراسات العليا، في جامعة النجاح الوطنية، نابلس– فلسطين.

2024

# نمذجة جريان المياه في مستجمع وادي الزيمار مع الأخذ في الاعتبار التغير المناخي

**إعداد**
**شهد عبد الحكيم يوسف بيشاوي**
**إشراف**
**د. محمد نهاد المصري**

## الملخص

تغطي المياه نسبة كبيرة من سطح الأرض، ولكن توافر المياه العذبة المناسبة للاستخدام البشري محدود. يركز العلماء على الهيدرولوجيا وإدارة الموارد المائية، مع استخدام النماذج الهيدرولوجية للتنبؤ بالتغيرات في موارد المياه. وتساعد النمذجة على فهم عمليات مثل هطول الأمطار. وفي مناطق مثل فلسطين، يمكن أن تؤدي العواصف الشديدة إلى حدوث فيضانات.

ويشكل تغير المناخ تحديا كبيرا، حيث يتوقع أن يؤدي ارتفاع درجات الحرارة العالمية إلى تغيير العمليات الهيدرولوجية، مما يزيد من تواتر حالات الجفاف والفيضانات. وللتصدي لمخاطر الفيضانات والتكيف مع هذه التغيرات، فإن فهم الاستجابة الهيدرولوجية لتغير المناخ في المستقبل أمر بالغ الأهمية. استخدمت هذه الدراسة نموذجاً هيدرولوجياً لوادي الزيمار في فلسطين مع إسقاطات مناخية لتقييم أثر اتجاهات المناخ في المستقبل على هيدرولوجيا مستجمعات المياه في واد الزيمار. حققت الدراسة نتائج موثوقاً بها بمعامل كفاءة ناش – سوتكليف قدره 0.863 وهذا يعطي انطباعا على أن النموذج يعطي نتائج ممتازة قريبة للواقع. تشير الإسقاطات المتعلقة بتغير المناخ إلى ارتفاع درجات الحرارة، وانخفاض معدلات هطول الأمطار، وزيادة الحد الأقصى لهطول الأمطار يوميا، مما يزيد من خطر حدوث الفيضانات المفاجئة.

وقد تنبأ تحليل الترددات بشأن الحد الأقصى للسقوط اليومي في محطة سقوط الأمطار في نابلس في الفترة من 1997 إلى 2022 بأقصى معدل للجري يبلغ 92 متراً مكعباً/ثانية بالنسبة لحدث فترة عودته 25 عاماً يتعلق ، مما استلزم إعادة تصميم عبارة واحدة فقط عند مدخل بلدة عنبتا كنموذج .

وتم توسيع العبارة، التي كان حجمها في البداية 10 أمتارا مربعة، إلى 30 مترا مربعا لتحمل شدة العاصفة المتوقعة. في النهاية , النموذج المبني يعطي نتائج ممتازة , والارقام تشير الى وجود كارثة حقيقية قد تواجه المنطقة , ويجب التوجه الى حلول غير توسيع العبارات.

**الكلمات المفتاحية:** الجريان السطحي , وادي الزيمار، التغير المناخي في فلسطين، النمذجة الهيدرولوجية